

RESEARCH ARTICLE

A Bayesian hierarchical model for disease mapping that accounts for scaling and heavy-tailed latent effects

Victoire Michal¹ | Laís Picinini Freitas² | Alexandra M. Schmidt*¹

¹Department of Epidemiology, Biostatistics and Occupational Health, McGill University, Montreal, Canada

²Programa de Computação Científica, Fundação Oswaldo Cruz, Rio de Janeiro, Brazil

Correspondence

*Alexandra M. Schmidt, Email: alexandra.schmidt@mcgill.ca

Abstract

In disease mapping, the relative risk of a disease is commonly estimated across different areas within a region of interest. The number of cases in an area is often assumed to follow a Poisson distribution whose mean is decomposed as the product between an offset and the logarithm of the disease's relative risk. The log risk may be written as the sum of fixed effects and latent random effects. The commonly used BYM model further decomposes the latent effects into a sum of independent effects and spatial effects to account for potential overdispersion and a spatial correlation structure among the counts. However, this model suffers from an identifiability issue. The BYM2 model reparametrises the latter by decomposing each latent effect into a weighted sum of independent and spatial effects. We build on the BYM2 model to allow for heavy-tailed latent effects and accommodate potentially outlying risks, after accounting for the fixed effects. We assume a scale mixture structure wherein the variance of the latent process changes across areas and allows for outlier identification. We explore two prior specifications of this scale mixture structure in simulation studies and in the analysis of Zika cases from the 2015-2016 epidemic in Rio de Janeiro. The simulation studies show that, in terms of WAIC and outlier detection, the two parametrisations always perform well compared to commonly used models. Our analysis of Zika cases finds 19 districts of Rio as potential outliers, after accounting for the socio-development index, which may help prioritise interventions.

KEYWORDS:

BYM2 model, Outliers, Scale mixture, Spatial statistics, Vector-borne disease, Zika virus infection

1 | MOTIVATION

The first Zika cases in the Americas were identified in 2015, when it was considered a benign disease. However, in October 2015 an unprecedented increase in the number of microcephaly cases in neonates was reported in the Northeast of Brazil and was later associated with the Zika virus infection during pregnancy¹. The Zika virus is transmitted to humans by the bite of infected *Aedes* mosquitoes, the same vectors that transmit dengue, chikungunya and yellow fever. Dengue is the most prevalent *Aedes*-borne disease in the world and around 3.9 billion people in 129 countries are at risk of acquiring the disease². Because of climate change, the global distribution of *Aedes* mosquitoes is expanding, increasing the number of people exposed to *Aedes*-borne diseases. In a recent study, researchers predict that more than 8 billion people could be at risk of dengue by 2080³.

In the city of Rio de Janeiro, Brazil, the first Zika epidemic occurred between 2015 and 2016, with more than 35 thousand confirmed cases⁴. The city is the second-largest in Brazil, with approximately 6.3 million inhabitants, and its main tourist destination. Rio de Janeiro has a tropical climate and a favourable environment for the *Ae. aegypti* mosquitoes, which are highly adapted to urban settings. Despite efforts to control the vector population, the city has suffered from dengue epidemics every three to four years, in general^{5,6,7}. The widespread presence of the mosquito also allowed the entry and rapid dispersion of Zika and chikungunya viruses⁴. This epidemiological scenario highlights the need for novel strategies to help design interventions that are more effective in decreasing the burden of established *Aedes*-borne diseases and preventing emerging and re-emerging arboviruses from causing new outbreaks. In this sense, we propose a model that has the potential to help prioritise interventions by identifying areas with outlying risks with respect to the entire region while accounting for covariates.

Motivating the proposed model, we have available the Zika cases counts aggregated by neighbourhood for the period of the first Zika epidemic in Rio de Janeiro city. The data come from the Brazilian Notifiable Diseases Information System (SINAN – *Sistema de Informação de Agravos de Notificação*). In Brazil, cases attending healthcare facilities with a suspected diagnosis of Zika are reported to this system, usually by the physician. The standardised morbidity ratios (SMR) for the Zika counts by neighbourhoods during the study period are presented in Figure 1. Although the epidemic affected most of the city, some neighbourhoods seem to have been hit harder than others. The diversity of the territory of Rio de Janeiro is possibly an important factor influencing this. Rio's territory is heterogeneous in terms of demographic, socio-economic, and environmental characteristics that are involved in the distribution of *Aedes*-borne diseases⁸.

For this analysis, we have available the socio-development index, an index that includes indicators related to sanitation, education and income, and for which higher values represent better socio-economic conditions. In places with inadequate sanitary conditions, the female *Ae. aegypti* can more easily find any type of container filled with water to deposit her eggs. In Rio de Janeiro, a very unequal city, the socio-development index ranges from 0.282 (in Grumari, a neighbourhood in the West region) to 0.819 (in Lagoa, South region)⁹. In a previous study from our group, the socio-development index presented a strong inverse association with the spatio-temporal distribution of chikungunya cases in Rio de Janeiro⁸.

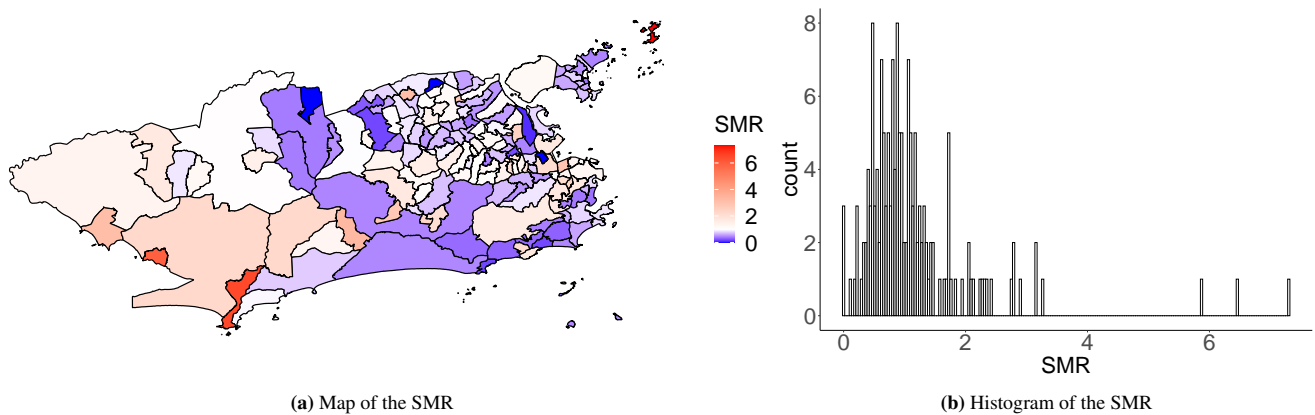


FIGURE 1 SMR for the Zika counts across the 160 neighbourhoods of Rio de Janeiro, 2015-2016.

1.1 | Literature review

In the last 30 years, the area of disease mapping has experienced an enormous growth. This is because it is an important tool for decision makers to obtain reliable areal estimates of disease rates over a region of interest. Disease mapping methods further help understanding the underlying associations between covariates and the disease risk. Commonly, Bayesian hierarchical models are used to model the disease cases observed in different areas that form a region of interest. The number of cases in an area is assumed to follow a Poisson distribution whose mean is decomposed as the product of an offset by the relative risk of the disease. Further, in the log scale, the relative risk is decomposed as the sum of covariates and latent (unobserved) areal effects. The latent

components also accommodate overdispersion as this decomposition of the log-relative risk can be seen as a Poisson-lognormal mixture model.

Usually, these latent effects follow a spatial structure, *a priori*, such that neighbouring locations will adjust in a similar fashion after accounting for the available covariates. Indeed, it seems natural to expect that areas that are close to each other are more correlated than areas that are further apart. However, some areas may present outlying risks that decision makers might want to identify after accounting for covariates. This issue of spatial heteroscedasticity has been increasingly considered over the recent years. For instance, regarding geostatistical data, Palacios and Steel¹⁰ proposed a log-normal scale mixture of a Gaussian process to accommodate heavy tails. In disease mapping, Congdon¹¹ also considered a scaling mixture model to adjust for locally outlying areas. In this model, the mixture parameters are assumed to follow a Gamma distribution *a priori* with mean 1 such that no overdispersion is assumed on average *a priori*. The scale mixture parameters introduced by Congdon¹¹ allow for identification of the areas that are different from their neighbours. More recently, in social geography, Dean et al.¹² addressed these local discrepancies termed "social frontiers" by changing the neighbouring structure according to the observed data. The authors study the proportion of non-UK population in the neighbourhoods of Sheffield in England. They first test for statistical differences between the observed proportions in neighbouring areas. When two neighbouring proportions are found to be statistically different, the spatial structure is updated such that the two areas are not considered as neighbours. This approach differs from Congdon's as it is a two-step procedure that implies changing the neighbourhood structure. Congdon¹¹, on the other hand, introduces scaling mixture parameters in order to deal with spatial discrepancies. In this paper, we are interested in identifying areas with outlying risks with respect to the entire region, after accounting for the effect of covariates. Decision makers may be interested in detecting these outliers in order to understand the disease distribution and prioritise interventions.

A commonly used spatial model for the latent effects that does not accommodate outliers is the conditional auto-regressive (CAR) prior¹³. Let $\mathbf{b} = [b_1, \dots, b_n]^\top$ be the vector of latent effects for the n areas of the region of interest. Under the CAR prior distribution, it is assumed that

$$b_i | \mathbf{b}_{(-i)}, \sigma_b^2 \sim \mathcal{N}\left(\frac{1}{d_i} \sum_{j=1}^n w_{ij} b_j, \frac{\sigma_b^2}{d_i}\right), \quad i = 1, \dots, n, \quad (1)$$

where $\mathbf{b}_{(-i)} = [b_1, \dots, b_{i-1}, b_{i+1}, \dots, b_n]^\top$, $\mathbf{W} = [w_{ij}]$ is the $n \times n$ matrix of weights, w_{ij} , that defines the neighbourhood structure and where $d_i = \sum_{j=1}^n w_{ij}$. Note that σ_b^2 is the variance of the *conditional distribution* of b_i given its neighbours. It can be shown¹⁴ that the joint distribution of \mathbf{b} is proportional to $p(\mathbf{b}) \propto \exp[-(1/2\sigma_b^2)\mathbf{b}^\top \mathbf{Q} \mathbf{b}]$, with $\mathbf{Q} = \mathbf{D} - \mathbf{W}$, where $\mathbf{D} = \text{diag}(d_i)$. To ease notation, let $\mathbf{b} \sim \mathcal{N}(\mathbf{0}, \sigma_b^2 \mathbf{Q}^-)$, where \mathbf{Q}^- is the generalised inverse of \mathbf{Q} . The CAR distribution is not a proper multivariate normal distribution as the "precision" matrix, \mathbf{Q} , is not positive definite. One issue with the CAR model is that it does not perform well when there is no underlying spatial structure in the data¹⁵.

To accommodate the presence of independent latent effects, Besag et al.¹⁶ proposed the so-called BYM model, where each areal latent effect, b_i , is decomposed as the sum of an unstructured component, θ_i , and a spatially structured component, u_i :

$$b_i = u_i + \theta_i, \quad i = 1, \dots, n, \quad (2)$$

with $\boldsymbol{\theta} = [\theta_1, \dots, \theta_n]^\top \sim \mathcal{N}(\mathbf{0}, \sigma_\theta^2 \mathbf{I})$, where \mathbf{I} is the n -dimensional identity matrix, independent from $\mathbf{u} = [u_1, \dots, u_n]^\top \sim \mathcal{N}(\mathbf{0}, \sigma_u^2 \mathbf{Q}^-)$, where σ_θ^2 is the variance of the *marginal distribution* of the unstructured components and σ_u^2 is the variance of the *conditional distribution* of the spatially structured components. As pointed out by MacNab¹⁷, this model presents an identifiability issue as the two variance components cannot be distinguished.

To avoid the introduction of two random effects for each area, Leroux et al.¹⁸ proposed an alternative distribution for the latent spatial effects that includes a spatial dependence parameter, λ . The latter is a mixing parameter in the unit interval that allows the variance of the latent effects to be decomposed into a weighted sum between an unstructured and a spatially structured variance components. The conditional distribution of each latent effect has the following form:

$$b_i | \mathbf{b}_{(-i)}, \lambda, \tau^2 \sim \mathcal{N}\left(\frac{\lambda}{1 - \lambda + \lambda d_i} \sum_{j=1}^n w_{ij} b_j, \frac{\tau^2}{1 - \lambda + \lambda d_i}\right), \quad i = 1, \dots, n, \quad (3)$$

where τ^2 is again the variance of the *conditional distribution* of b_i given its neighbours. This prior is a proper distribution for all $\lambda \in [0, 1)$.

Sørbye and Rue¹⁹ argued that scaling spatially structured effects is essential to ease interpretation and prior assignment of the variance parameter of the latent effects, independently of the neighbourhood structure. Best et al.²⁰ discuss this sensitivity to prior assignments regarding the BYM model. Indeed, the parameters involved in the prior distribution of the latent effects are often incorrectly interpreted as the properties of the marginal distribution of \mathbf{b} . These actually depend on the neighbourhood

structure and do not have the same meaning in every data application. Hence, to overcome this issue, Riebler et al.²¹ proposed the BYM2 model, that decomposes the latent effects into a weighted sum of unstructured random noises with unit variance and scaled structured components. The vector of latent spatial effects is scaled according to the neighbourhood structure. The decomposition of the i th latent effect is as follows:

$$b_i = \sigma \left(\sqrt{1 - \lambda} \theta_i + \sqrt{\lambda} u_i^* \right), \quad i = 1, \dots, n, \quad (4)$$

where $\lambda \in [0, 1]$ and $\theta \sim \mathcal{N}(\mathbf{0}, \mathbf{I})$ is independent from the scaled spatially structured components, $\mathbf{u}^* = [u_1^*, \dots, u_n^*]^\top \sim \mathcal{N}(\mathbf{0}, \mathbf{Q}_*^-)$. The matrix \mathbf{Q}_*^- is the generalised inverse of \mathbf{Q}_* , which is a scaled version of the CAR "precision" matrix, $\mathbf{Q}: \mathbf{Q}_* = h\mathbf{Q}$. The scaling factor, h , is proportional to the generalised variance that arises from a CAR model: $h = \exp \left[(1/n) \sum_{i=1}^n \ln(\mathbf{Q}_{ii}^-) \right]$. Note that the scaling factor only depends on the neighbourhood structure. This scaled CAR prior corresponds to $\mathbf{u}^* = [u_1/\sqrt{h}, \dots, u_n/\sqrt{h}]^\top$, for $\mathbf{u} \sim \mathcal{N}(\mathbf{0}, \mathbf{Q}^-)$. As stated by Sørbye and Rue¹⁹, this scaling process allows each structured component to have a variance of approximately 1. It results that $\mathbb{V}(b_i | \sigma) \simeq \sigma^2 [(1 - \lambda) \times 1 + \lambda \times 1] = \sigma^2$. Hence, a *marginal* variance, σ^2 , is defined for the latent effects and all the parameters can be interpreted for all neighbourhood structures.

On the other hand, spatial heteroscedasticity is not explicitly considered in the previous models. However, it is reasonable to imagine that some areas may have abnormally high or low disease risks. The goal of this paper is to propose a method to accommodate and identify outlying areas. To capture outliers, Yan²² proposed a double CAR model, where the relative risk is decomposed into the sum of a CAR spatial effect and an additional noise whose variance is modelled, in the log scale, through a BYM prior. Congdon¹¹ argued that this model formulation may lead to identifiability issues, as the three sets of latent effects may not be distinguishable. To allow for local disparities, Congdon¹¹ proposed a modification of the Leroux prior by including scale mixture parameters. More specifically, Congdon¹¹ assumes

$$b_i | \mathbf{b}_{(-i)}, \boldsymbol{\kappa}, \lambda, \tau^2 \sim \mathcal{N} \left(\frac{\lambda}{1 - \lambda + \lambda d_i} \sum_{j=1}^n w_{ij} \kappa_j b_j, \frac{\tau^2}{\kappa_i (1 - \lambda + \lambda d_i)} \right), \quad i = 1, \dots, n, \quad (5)$$

with $\kappa_i \stackrel{i.i.d.}{\sim} \text{Gamma}(\nu/2, \nu/2)$, $i = 1, \dots, n$ and $\nu \sim \text{Exp}(1/\mu_\nu)$, for some value of μ_ν fixed by the analyst. These positive parameters, $\boldsymbol{\kappa} = [\kappa_1, \dots, \kappa_n]^\top$, allow for discrepancies in the neighbouring estimated risks, while the usual CAR-type priors aim to locally smooth the risk surface. The scale mixture parameters are termed outlier indicators as $\kappa < 1$ captures local outliers, namely areas that have different rates from their neighbours. Again, τ^2 is the variance of the *conditional distribution* of b_i given its neighbours. This implies that the interpretation of τ^2 differs with every spatial structure and its prior distribution should be defined with care for every data application. It can be shown¹¹ that the joint distribution of the latent effects is $\mathbf{b} | \tau^2, \lambda, \boldsymbol{\kappa} \sim \mathcal{N}(\mathbf{0}, \tau^2 \mathbf{Q}_C^-)$, where the "precision" matrix has diagonal elements $\mathbf{Q}_{C_{ii}} = \kappa_i (1 - \lambda + \lambda d_i)$ and off-diagonal elements $\mathbf{Q}_{C_{ij}} = -\lambda w_{ij} \kappa_i \kappa_j$. The diagonal dominance condition²³ states that a sufficient condition for a symmetric matrix \mathbf{Q}_C to be symmetric positive definite is $\mathbf{Q}_{C_{ii}} > \sum_{j \neq i} |\mathbf{Q}_{C_{ij}}|$, $\forall i$. Hence, it is sufficient that $\lambda \in (0, 1)$ and $\lambda < \min_i \{1 / (1 - d_i + \sum_{j \neq i} w_{ij} \kappa_j)\}$, for \mathbf{Q}_C to be a valid precision matrix. Note that if $\boldsymbol{\kappa} = \mathbf{1}_n$, then Congdon's prior is the Leroux prior, which is proper for $\lambda \in [0, 1)$. This mixture differs from the commonly used normal-gamma model as the scale mixture components appear both in the mean and in the variance of the conditional distribution.

In this paper, we propose a modification of the BYM2 prior²¹ that is able to identify areas with outlying disease risks, after accounting for the effect of covariates. A scale mixture is introduced in the variance of the BYM2 model as in Congdon¹¹. The proposed model keeps the appealing property of parameter interpretation while capturing and identifying potentially outlying areas. This paper is organised as follows: Section 2 describes the proposed model with the proposed decomposition of the latent effects. A simulation study showcases the performance of the proposed model in section 3 under different scenarios. Additionally, the application of the proposed model to the data presented in section 1 from the 2015-2016 Zika epidemic in the 160 neighbourhoods of Rio de Janeiro is shown in section 3. We conclude by a discussion in section 4.

2 | PROPOSED MODEL

Let a region of interest be partitioned into n non-intersecting areas. Let Y_i be the number of cases in area i , $i = 1, \dots, n$, and E_i , the expected number at risk in that area. The counts are modelled through the following Poisson model:

$$Y_i | E_i, \mu_i \sim \mathcal{P}(E_i \mu_i),$$

where μ_i denotes the relative risk in area i and E_i is an offset. Commonly, the risk is decomposed in the log scale as follows:

$$\ln(\mu_i) = \beta_0 + \mathbf{x}_i \boldsymbol{\beta} + b_i,$$

where β_0 is the mean log risk, \mathbf{x}_i is a p -dimensional vector with the explanatory variables in area i , associated with the p coefficients $\boldsymbol{\beta}$, and b_i is a random effect for area i . The latter is included in order to allow for overdispersion in the Poisson model that would otherwise assume equal mean and variance for area i . The latent areal effects can also accommodate an assumed underlying spatial structure in the data. To that end, a spatial structure is defined through the matrix $\mathbf{W} = [w_{ij}]$. Throughout this paper, we assume that two areas are said to be neighbours if they share a border. This implies that $w_{ij} = 1$ if areas i and j are neighbours and $w_{ij} = 0$, otherwise. In this setting, $d_i = \sum_{j=1}^n w_{ij}$ corresponds to the number of neighbours of area i . To model the latent areal effects accounting for such 0-1 spatial structure, we propose a modification of the prior specification (4) proposed by Riebler et al.²¹, that is, we assume

$$b_i = \frac{\sigma}{\sqrt{\kappa_i}} \left(\sqrt{1 - \lambda} \theta_i + \sqrt{\lambda} u_i^* \right), \quad i = 1, \dots, n, \quad (6)$$

where $\sigma > 0$ is scaled by $\kappa_i > 0$, and where $\lambda \in [0, 1]$. The component θ_i is assumed independent from u_i^* . In particular, $\boldsymbol{\theta} \equiv [\theta_1, \dots, \theta_n]^\top \sim \mathcal{N}(\mathbf{0}, \mathbf{I})$, and $\mathbf{u}^* \equiv [u_1^*, \dots, u_n^*]^\top \sim \mathcal{N}(\mathbf{0}, \mathbf{Q}_\star^-)$. The latter two are termed the unstructured and the scaled structured components, respectively. Like in the BYM2 model²¹ (4), the "precision" matrix is such that $\mathbf{Q}_\star = h\mathbf{Q}$, where the scaling factor, h , is computed from the neighbourhood structure (see section 1.1). It results that $\mathbb{V}(b_i \mid \sigma, \kappa_i) \simeq (\sigma^2/\kappa_i) [(1 - \lambda) \times 1 + \lambda \times 1] = \sigma^2/\kappa_i$. Hence, σ^2/κ_i represents the approximate *marginal* variance of the latent effect of area i . Moreover, the variance-covariance matrix, \mathbf{V} , of the proposed latent effects, \mathbf{b} , is given by $\mathbf{V} = \sigma^2 \mathbf{K}^{-1} [(1 - \lambda)\mathbf{I} + \lambda \mathbf{Q}_\star^-]$, where $\mathbf{K} = \text{diag}(\kappa_i)$. Thus, the parameter λ represents the weight of the spatial effect in the variance of the latent process. Note that this distribution is a proper multivariate normal for small values of λ , depending on the neighbourhood structure. Indeed, the diagonal dominance condition²³ implies that it is sufficient that $\lambda \in [0, 1]$ and $\lambda < \min_i \left\{ 1 / \left(1 - \mathbf{Q}_{\star ii}^- + \sum_{j \neq i} |\mathbf{Q}_{\star ij}^-| \right) \right\}$ for the covariance matrix, \mathbf{V} , to be valid.

In a nutshell, the proposed model uses interpretable parameters to accommodate outlying areas while identifying them. The proposed model points at neighbourhoods that need heavy-tailed latent effects after accounting for some covariates. Different from Congdon¹¹ (5), the proposed model introduces parameters that intervene on the *marginal* distribution of the latent effects. Therefore, their interpretation remains the same for any spatial structure and the prior assignment is simplified. This concerns the marginal variance, σ^2 , as well as the scaling mixture parameters, $\boldsymbol{\kappa} = [\kappa_1, \dots, \kappa_n]^\top$.

2.1 | Prior specification of the scale mixture component

Different priors may be considered for the scale mixture components, $\boldsymbol{\kappa}$. A natural choice, and used by Congdon¹¹, is to assume:

$$\kappa_i \stackrel{i.i.d.}{\sim} \text{Gamma}(\nu/2, \nu/2), \quad i = 1, \dots, n, \quad \text{and} \quad \nu \sim \text{Exp}(1/\mu_\nu), \quad (7)$$

where the hyperparameter's mean, μ_ν controls the magnitude of ν . When $\lambda = 0$, and marginalising the proposed distribution (6) of the latent effect, b_i , with respect to κ_i yields a t_{μ_ν} . The introduction of κ_i hence allows for heavier tails than a Gaussian distribution for the latent effects. In this case, μ_ν corresponds to choosing the prior distribution of the degrees of freedom of the resulting t distribution which impact the moments of the distribution as well as its tails. A large μ_ν results in a distribution very close to being normal, which is inadequate to capture outliers. On the other hand, $\mu_\nu < 3$ implies a t distribution whose variance is not defined. Some simulation studies showed that setting $\mu_\nu = 4$ performed well, which agrees with Gelman et al.²⁴.

The above prior specification (7) is the same one used by Congdon¹¹. In Congdon's model, the κ 's contribute with two aspects to the *conditional* distribution of the latent effects: in the mean and in the variance. To visualise the κ 's impacts in Congdon's model, say $\kappa_i < 1$ for $i \sim j$, that is for neighbouring areas i and j . First, as κ_i appears in the conditional mean structure of the latent effect for area j , the weight of area i is decreased and area i contributes less to the mean of the j th latent effect than its other neighbours. Second, by being part of the variance structure, $\kappa_i < 1$ gives area i an increased variability and thus allows it to differ from its neighbours. On the other hand, in the proposed model, the κ 's only intervene on the *marginal* variances. Therefore, $\kappa_i < 1$ acts as an outlier indicator for the random effect of area i with respect to the whole region of interest by increasing its variability and hence allowing it to differ from the overall mean structure.

Another possible prior specification for the κ 's is to borrow ideas from Palacios and Steel¹⁰ who proposed the inclusion of a scale mixture component in the variance of a Gaussian process. The authors suggest the usual gamma mixing is not always appropriate as not all positive moments exist. Additionally, they point out that the t distribution that results from marginalising over the gamma scaling mixture parameters may still overestimate the overall variance and struggle to detect specific outlying areas. In particular, they assume that the scale mixture component follows a log-Gaussian process with the same spatial structure as the one defined for the main Gaussian process. In our proposed model, we assume a scaled log-CAR prior distribution for the κ 's. This form of discretisation of the method proposed by Palacios and Steel¹⁰ is applied to the latent effects, which include both the structured and unstructured components, in order to keep the interpretative property of the parameters. This contrasts with the method proposed by Palacios and Steel¹⁰ as they introduced a scale mixture only for the spatially dependent components. The scale mixture components are modelled as follows:

$$\ln(\kappa_i) \equiv -\frac{\nu_\kappa}{2} + z_i, \quad i = 1, \dots, n, \quad (8)$$

where $\mathbf{z} \equiv [z_1, \dots, z_n]^\top \mid \nu_\kappa \sim \mathcal{N}(\mathbf{0}, \nu_\kappa \mathbf{Q}_\star^-)$ and $\nu_\kappa \sim \text{Exp}(1/\mu_{\nu_\kappa})$,

where $\mathbf{Q}_\star = h\mathbf{Q}$ is again the "precision" matrix that is scaled by h , which is computed according to the spatial structure. The CAR distribution is scaled in order to approximately have that $\mathbb{V}[\ln(\kappa_i) \mid \nu_\kappa] \simeq \nu_\kappa \times 1$. This distribution is not a proper distribution since \mathbf{Q}_\star is not of full rank. Similarly to Palacios and Steel¹⁰, this prior implies $\mathbb{E}(\kappa_i \mid \nu_\kappa) \simeq 1$, which corresponds to a constant marginal variance across the areal latent effects, and $\mathbb{V}(\kappa_i \mid \nu_\kappa) \simeq \exp(\nu_\kappa) - 1$, $\forall i$. For ν_κ close to 0, κ is close to 1 with a small variance. A bigger ν_κ allows the κ 's to differ greatly from 1 and to be closer to 0, when necessary. As before, smaller values of κ_i increase the latent variance for area i and again, $\kappa_i < 1$ indicates that area i is a potential outlier. Palacios and Steel¹⁰ suggest that a reasonable prior mean for ν_κ is $\mu_{\nu_\kappa} = 0.2$. The many simulation studies we conducted suggest that a sensible choice for μ_{ν_κ} is $\mu_{\nu_\kappa} = 0.3$ as it yields $[0.2, 2.4]$ as the 95% prior credible interval for the κ 's. This includes $\kappa_i = 1$ while allowing for departure from $\kappa_i = 1$, to accommodate the potentially outlying random effect of area i . This prior specification for the κ 's allows for a detection of outlying areas with respect to the whole region of interest while also accommodating local discrepancies thanks to the inclusion of the spatial structure, \mathbf{Q} .

2.2 | Inference procedure

Following the specifications discussed in the previous section the resultant posterior distribution, regardless of the prior specification for κ_i does have closed analytical form. Therefore, the resultant posterior distributions are approximated through computational methods. In particular, Markov Chain Monte Carlo (MCMC) methods are considered. The Hamiltonian Monte Carlo method implemented in the R package `rstan`²⁵ is used for the simulation studies and real data application that follow. Morris et al.²⁶ note that the No U-Turn Sampler implemented in `rstan` is more efficient than other MCMC samplers to obtain reliable estimates of the posterior distributions induced by the complex auto-regressive type of models that are of interest in this paper.

One way to approximate a proper posterior distribution when assigning a CAR prior, is to add a sum-to-zero constraint on the parameters in order to distinguish them from any added constant. This is necessary due to the invariance of the CAR distribution to the addition of a constant²³. The sum-to-zero constraint is applied to the spatial components of the proposed model, \mathbf{u} , that need to be distinguished from the global intercept, β_0 , as well as for the log-CAR scale mixture components, where $\ln(\mathbf{z})$ must be different from the mean $-\nu_\kappa/2$. More precisely, we add a soft sum-to-zero constraint in both cases, that is $\sum_{i=1}^n u_i \sim \mathcal{N}(0, n/1000)$ and $\sum_{i=1}^n \log(z_i) \sim \mathcal{N}(0, n/1000)$, respectively. The `rstan` implementation of the BYM2 model is discussed by Morris et al.²⁶ and the code for the proposed model, which is a modification of the BYM2, is available in Appendix A.

The scaling factor, h , needed in the BYM2 and, hence, in the proposed model is computed through the R package `R-INLA` (Integrated Laplace Approximation, Rue et al.²⁷, www.r-inla.org) as explained by Riebler et al.²¹.

3 | DATA ANALYSES

In this section, we present the results of one of the many simulation studies that were conducted and fit the proposed model to data obtained from the first Zika epidemic that took place in 2015 and 2016 in Rio de Janeiro. In both cases, we consider the two parametrisations of the proposed model, which correspond to the two prior specifications of the scaling mixture components

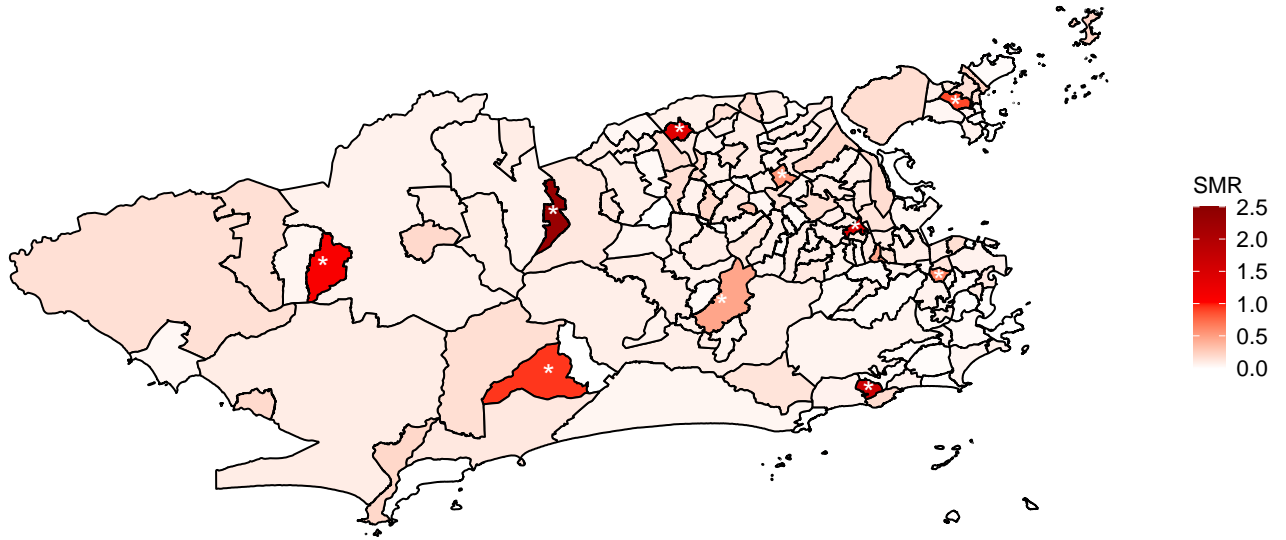


FIGURE 2 Standardised morbidity ratio (SMR= Y/E) for the 50th simulation. *: contaminated districts

described in section 2.1. First, in the simulation study, we generate data for the 160 districts of Rio de Janeiro and contaminate 10 areas. The goal is to check if our proposed model is able to identify these 10 generated outliers. We compare the performance of the two parametrisations of the proposed model to the one from Congdon¹¹. Second, in the Zika data application, we compare the results of our proposed model to Congdon's as well as the BYM2²¹ and Leroux¹⁸ models. We identify some potentially outlying districts which might be of interest to decision makers.

3.1 | Simulation study

To assess the performance of the proposed model, many simulation studies are conducted. First, in Appendix C and in Appendix D, two simulation studies show the ability of the two versions of the proposed model to recover the true parameters when data are generated from the model itself. Then, Appendix E presents a simulation study without any outlying areas which results in the proposed model performing well compared to the prior by Congdon¹¹. Here we present the results from a simulation study wherein some areas are contaminated into outlying areas, to compare the performance of the proposed model in comparison to the one proposed by Congdon. The $n = 160$ districts of Rio de Janeiro and their neighbourhood structure are used as the region of study.

First, the latent effects are simulated according to a proper CAR model, denoted PCAR hereafter: $\mathbf{b} \sim \mathcal{N}(\mathbf{0}, \sigma_b^2[\mathbf{D} - \alpha\mathbf{W}]^{-1})$, with α and σ_b arbitrarily set to 0.7 and $\sqrt{0.7}$, respectively. Note that the parameter α is reasonably small as $\alpha = 1$ corresponds to a CAR prior, wherein the spatial structure is essential, while $\alpha = 0$ produces independent random effects with variances proportional to the inverse of the number of neighbours. Then, 10 far apart districts are contaminated; namely Estácio, Vila Kosmos, Jardim Carioca, Costa Barros, Freguesia (Jacarepaguá), Vargem Pequena, Padre Miguel, Inhoaíba, Rocinha and Jacarezinho. The number of cases are contaminated by adding random uniform values to the initially generated PCAR latent effects. Finally, using the contaminated effects, \mathbf{b} , 100 populations of size $n = 160$ are created, according to a hierarchical Poisson model. That is, $Y_i \sim \mathcal{P}(E_i \exp[\beta_0 + \beta x_i + b_i])$, with $\beta_0 = -0.1$, $\beta = -4$ and the offsets, $[E_1, \dots, E_n]^\top$, and covariates, $[x_1, \dots, x_n]^\top$, taken from the real data application to the Zika counts that is presented in section 3.2. The only source of randomness across the 100 replicates comes from the repeated sampling from a Poisson distribution. Indeed, the spatial effects are generated only once and are considered as fixed. The standardised morbidity ratios, Y/E , for the 50th simulation are mapped in Figure 2.

The Congdon prior is compared to the proposed model with the two scale mixtures described in section 2.1. The first version of the proposed model is denoted BYM2-Gamma and the second, BYM2-logCAR. For the three models, the intercept and

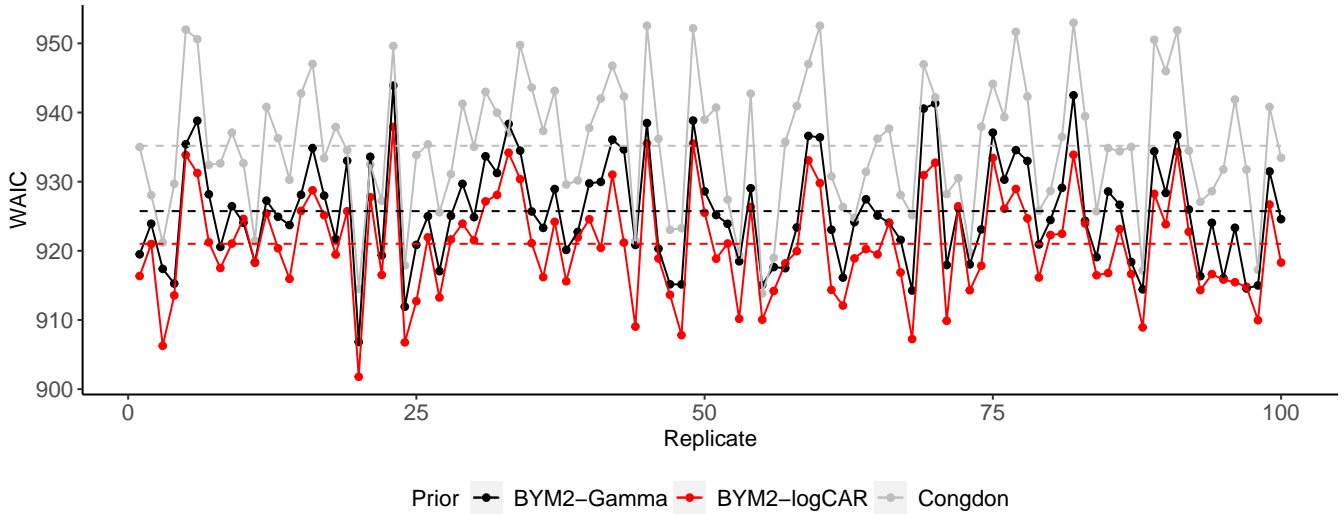


FIGURE 3 WAIC across the 100 replicates for the proposed models and Congdon's. Dashed lines: mean WAIC for each model

regression coefficient are given a quite vague prior: $\beta_0, \beta \stackrel{i.i.d.}{\sim} \mathcal{N}(0, 10^2)$ and the mixing parameter, λ , is assigned a uniform, $\mathcal{U}(0, 1)$, prior distribution. The same fairly informative $\mathcal{N}_+(0, 1)$ prior is considered for σ , which is a *marginal* standard deviation in the proposed model, while it is a *conditional* standard deviation in Congdon's. Finally, in the BYM2-Gamma and Congdon models, we set *a priori* that $\kappa_i \stackrel{i.i.d.}{\sim} \text{Gamma}(\nu/2, \nu/2)$ and $\nu \sim \text{Exp}(1/4)$. For the BYM2-logCAR parametrisation of the proposed model, we set $\ln(\kappa) = -(\nu/2)\mathbf{1} + \mathbf{z}$, with $\mathbf{z} \mid \nu \sim \mathcal{N}(\mathbf{0}, \nu\mathbf{Q}_\star^-)$, where \mathbf{Q}_\star is defined through the neighbourhood structure of Rio de Janeiro and $\nu \sim \text{Exp}(1/0.3)$.

The models are fitted through the R package `rstan` (Stan Development Team, 2020) and the code to fit the proposed BYM2-Gamma model is available in Appendix A. For each dataset, the MCMC procedure consists of 2 chains of 20,000 iterations with a 10,000 burn-in period and a thinning factor of 10. Convergence of the chains is assessed through trace plots, effective sample sizes and the \hat{R} statistic (Gelman et al.²⁸, Vehtari et al.²⁹).

In terms of WAIC³⁰, for which smaller values are preferred, the proposed models always perform better than Congdon's, as shown in Figure 3. On average, the BYM2-logCAR model yields a criterion of 921.0, the BYM2-Gamma model presents a WAIC of 925.7, versus 935.2 for Congdon's.

Figure 4 and Figure 5 summarise the inference for the parameters $\beta_0, \beta, \lambda, \nu$ and σ for the three models across the 100 replicates. The posterior means (solid circles) and posterior 95% credible intervals (vertical lines) are shown for every parameter for each model across the 100 replicates. All models recover the true intercept and the true coefficient β as shown in Figure 4. In Figure 5, for the hyperparameter of the scaling mixture, ν , the results cannot be directly compared between the BYM2-logCAR model and the two others as ν does not play the same role under the different parametrisations. Both the BYM2-Gamma and Congdon's models lead to similar results. Note that for the latter two, there seems to be enough information in the data to learn about this higher level parameter as the posterior summaries differ from the prior mean of 4 with prior 95% credible interval, [0.1, 14.7]. The same comment applies to the hyperparameter in the BYM2-logCAR model: the credible bounds go from [0.0, 1.1] *a priori* to [0.6, 2.5] on average *a posteriori*. Regarding the mixing parameter, λ , the two versions of the proposed model estimate it to be smaller than Congdon's. In fact, λ is not directly comparable between Congdon's and the proposed models. In Congdon's model, λ represents the weight of the spatial structure on the means and variances of the *conditional* distributions of the latent effects, while it corresponds to the overall weight of the spatial structure on the *marginal* distribution of the latent effects in the proposed model. Thus, Congdon's model points on average to a 75% weight of the spatial structure for the *conditional* distributions of the latent effects and the two parametrisations of the proposed model indicate a fairly small spatial structure, *marginally*. This result is sensible for two reasons. First, as previously stated, the parameter $\alpha = 0.7$ is fairly small in the PCAR generating distribution of the spatial effects. Second, by introducing contamination, we reduce yet more the overall importance of the spatial structure in the data.

Again, a distinction needs to be made between the two parametrisations of the proposed model and Congdon's concerning the parameter σ , which appears in the *conditional* variance of the latent effects in Congdon's model and in the *marginal* one in

the proposed model. The BYM2-Gamma model estimates a small σ , which corresponds to the overall standard deviation that is common to all the districts. The true marginal standard deviation is then captured due to the inclusion of the κ 's that increase the areal variances only when necessary.

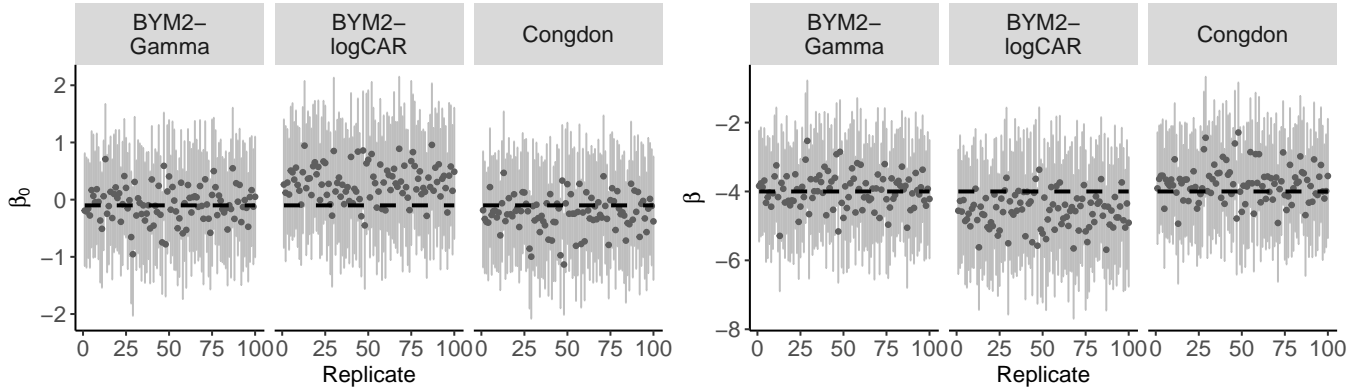


FIGURE 4 Posterior summaries of the model coefficients for the three models across the 100 replicates. Solid circle: posterior mean; Vertical lines: 95% posterior credible interval; Dashed horizontal line: true value.

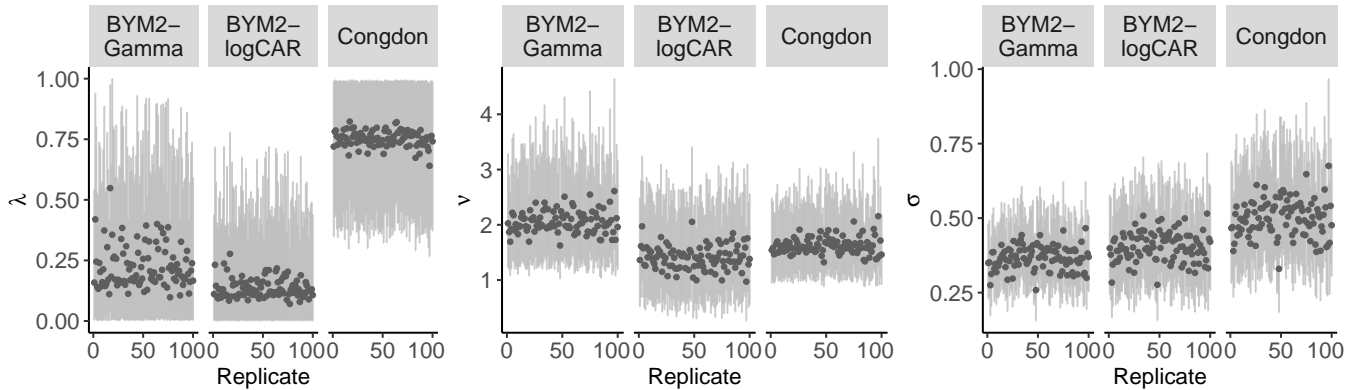


FIGURE 5 Posterior summaries of the model parameters for the three models across the 100 replicates. Solid circle: posterior mean; Vertical lines: 95% posterior credible interval.

Regarding the detection of outliers, which is the main focus of the proposed model, Figure 6 shows how often each district is detected as a potential outlier by the three models. Overall, all models are able to find the contaminated districts, as shown by the red areas that are indicated to have been contaminated by the white stars. However, the BYM2-logCAR model detects Vila Kosmos as an outlier only 83% of the time, which may be due to chance from the contamination process. The BYM2-Gamma version of the proposed model does not find any other outliers. The BYM2-logCAR parametrisation does identify the district of Tauá as an additional outlier in 21% of the replicates. This is probably due to the spatial structure that is induced in the scaling mixture components, as Tauá shares a border with Jardim Carioca, which is one of the 10 contaminated districts. Furthermore, Congdon's model often points two other districts as potential outliers, namely Senador Vasconcelos (68%) and Penha (24%). This tendency of Congdon's prior and, at a lower scale, the proposed BYM2-logCAR model to report more outliers than were generated was further explored in Appendix E. In the simulation study shown in Appendix E, data are generated from the hierarchical Poisson model with latent effects following a PCAR distribution and no district is contaminated. Hence, there are no outliers. This study reports that the proposed BYM2-Gamma model does not identify any district as an outlier whereas the

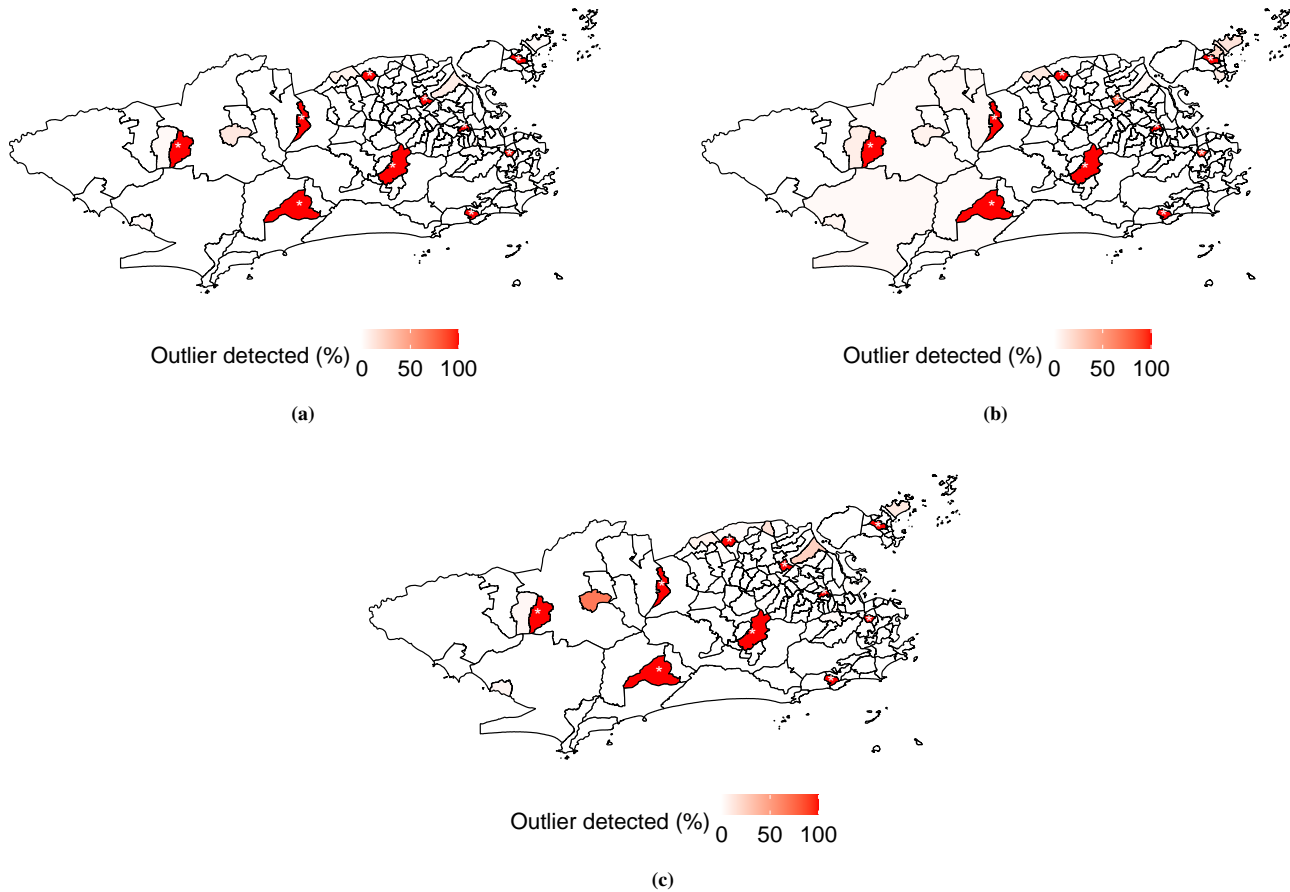


FIGURE 6 Maps of the outliers indicated by $\kappa_u < 1$, where κ_u is the upper bound of the posterior 95% credible interval of κ . a) BYM2-Gamma model; b) BYM2-logCAR model; c) Congdon's model.

proposed BYM2-logCAR model detects one district as a potential outlier in 8% of the replicates, showing a sensitivity to the neighbourhood structure. Furthermore, Congdon's model detects 6 districts as potential outliers up to 8% of the times, showing even more sensitivity to the neighbourhood structure.

Note that all models are able to recover the observed values. Therefore, in terms of fitted values, there is not a big difference among the models. However, the main advantage of the proposed model is its ability to identify areas with potentially outlying random effects while having interpretable parameters. This interpretability helps when specifying the prior distributions of the hyperparameters.

3.2 | Cases of Zika during the 2015-2016 epidemic in Rio de Janeiro

The total numbers of cases of Zika were recorded across the 160 neighbourhoods of Rio de Janeiro during the first epidemic, which took place between 2015 and 2016. Let Y_i be the disease count in district $i = 1, \dots, 160$. A hierarchical Poisson model is fitted to these data with offsets, E , computed from, P , the areal population sizes, $E_i = P_i (\sum_j Y_j / \sum_j P_j)$. We consider a socio-development index, x , as an explanatory variable for the number of cases. Identifying districts with potentially outlying risks, after accounting for covariates, may be useful for decision makers to understand how to prevent Zika and where to start from. The distribution of Zika is described through a map and a histogram of the standardised morbidity ratio (SMR), Y/E , in Figure 1 in section 1. Some districts seem to present different SMR values than the mean surface, such as the island Paquetá, Barra de Guaratiba and Pedra de Guaratiba, with SMRs of 7.3, 6.5 and 5.9, respectively. In the lower tail of the SMR distribution, three districts did not record any cases and thus present null SMRs, namely Gericinó, Vasco da Gama and Parque Colúmbia. However, the SMR being an exploratory tool, one cannot conclude that high or low SMR values necessarily indicate outlying districts.

Therefore, we are interested in comparing which districts are identified as potential outliers, after accounting for the socio-development index, by the two versions of the proposed model and Congdon's. The same priors are defined for the parameters as in the simulation study presented in section 3.1 and the two versions of the proposed model are again denoted BYM2-Gamma and BYM2-logCAR. We further compare the performance of the three models to the BYM2 and Leroux models which do not accommodate potential outliers.

All models are fitted in `rstan` (Stan Development Team, 2020) with 2 chains of 20,000 iterations thinned by 10 and of which 10,000 are burnt. As assessed by the trace plots, the effective sample sizes and the \hat{R} statistics²⁸, the two chains have mixed well for all five models and convergence is attained.

The results from the fitted models are presented in Table 1 and Figure 7. In terms of WAIC, the proposed BYM2-Gamma model performs best among the five considered. There is an important performance gain when accommodating outliers (BYM2-Gamma, BYM2-logCAR and Congdon: 1335, 1342 and 1337, respectively, vs BYM2 and Leroux: 1371 and 1375, respectively). Congdon's prior, that focuses on local outliers, does not seem to perform significantly worse than the BYM2-Gamma model, which concentrates on outliers with respect to the general distribution of the spatial effects. However, Congdon's model yields a smaller WAIC than the BYM2-logCAR proposed prior. Interestingly, even though the BYM2-Gamma model has 160 more parameters than Congdon's, its effective number of parameters is similar (80 vs 81).

Regarding the intercept, β_0 , the proposed models and Congdon's give similar results whereas the Leroux and BYM2 models yield smaller posterior means and lower credible interval bounds. This is probably due to the difference in the spatial effects that are allowed to be more extreme in the Congdon, BYM2-Gamma and BYM2-logCAR models. All five models indicate that richer districts have smaller risks of Zika (posterior means for β of -3 for the BYM2 and Leroux models and -4 for the proposed models and Congdon's). We cannot directly compare the parameters λ and σ between the BYM2-type models and Leroux-type priors as these appear in the *marginal* and *conditional* distributions of the latent effects, respectively. Marginally, the BYM2-type models yield similar weights of the spatially structured components on the latent effects (posterior means for λ of 0.6 and 0.7). However, a difference is noted between the Leroux-type models. The Leroux prior estimates λ to be very close to 0 (posterior credible interval of [0.00, 0.01]). This contrasts with the posterior credible interval of [0.5, 1.0] that results from fitting Congdon's model. This difference is probably due to the presence of outliers in the data, which results in the Leroux model finding more random noise in the latent effects. The same observation can be made for the marginal standard deviation, σ , regarding the BYM2-type models. The posterior credible interval for σ is significantly higher in the BYM2 model compared to the two parametrisations of the proposed model. Indeed, the proposed models are able to estimate a smaller overall variance for the latent effects which is then adjusted through the κ 's when needed. Finally, it can be noted that there is enough information in the data to learn about the hyperparameter ν . This parameter was assigned a prior mean of 4 and prior 95% credible interval of [0.1, 14.7] for the BYM2-Gamma and Congdon models and resulted in posterior means of about 2 and posterior 95% credible intervals of about [1, 3]. The BYM2-logCAR model assigned an exponential distribution with mean 0.3 for ν , inducing a prior 95% credible interval of [0.0, 1.1], and yielded a posterior credible interval of [0.7, 2.3], showing the need for some κ 's to be different from 1, *a posteriori*.

We now focus on the outliers detected by the proposed models and Congdon's, as shown in Figure 7. District i is again found to be a potential outlier, after accounting for the socio-development index, if the upper bound of the posterior 95% credible interval of κ_i is below 1. The detailed posterior summaries (posterior mean and posterior 95% credible interval) for the scale mixture components estimated in all three models can also be found in Table B1 in Appendix B. In Figure 7, the blue and red coloured districts help distinguish the detected outliers on the lower tail of the SMR distribution from the ones on the upper tail. After accounting for the socio-development index, some districts are pointed out by the three models, such as Gericinó, Parque Colúmbia, Vasco da Gama and Maré, on the lower tail of the SMR distribution, Barra de Guaratiba, Bonsucesso and Vista Alegre, on the upper tail. However, the BYM2-Gamma and Congdon's models both do not point out Paquetá in the upper tail whereas the BYM2-logCAR model detects it. Note, however, that the BYM2-Gamma model is close to identifying Paquetá as an outlier as it results in $\kappa_u = 1.04$ for this district, where κ_u denotes the upper bound of the 95% posterior credible interval. Figure B1 in Appendix B shows the posterior means for the latent effects obtained from all five models. Note that the BYM2 model and the Leroux prior, which do not accommodate heavy-tailed random effects, both estimate a high posterior mean for Paquetá's latent effect. This shows that there may be no need to allow for a higher random effect for this district. The three models do not identify Pedra de Guaratiba which has a high SMR, as shown in Figure 1. The BYM2-logCAR model is the closest to detecting it, with a κ_u of 1.09 for that district. Interestingly, the district of São Cristóvão is detected as an outlier by both the BYM2-logCAR and Congdon's models whereas it is not by the BYM2-Gamma model, with $\kappa_u = 1.2$. The BYM2-logCAR and Congdon's models detect more potential outliers than the BYM2-Gamma model as these may be more sensitive

	BYM2	BYM2-logCAR	BYM2-Gamma	Congdon	Leroux
Model fit					
WAIC	1371.2	1342.3	1335.6	1337.5	1375.1
p_W	88.6	82.3	80.0	81.0	89.2
Parameters' posterior summaries					
	Mean (95% CI)	Mean (95% CI)	Mean (95% CI)	Mean (95% CI)	Mean (95% CI)
β_0	1.6 (0.4,2.8)	2.5 (1.3,3.5)	2.5 (1.7,3.4)	2.4 (1.4,3.2)	1.6 (0.7,2.6)
β	-2.8 (-4.8,-0.8)	-4.2 (-5.8,-2.3)	-4.3 (-5.6,-2.9)	-4.0 (-5.4,-2.6)	-2.9 (-4.4,-1.3)
λ	0.7 (0.4,0.9)	0.6 (0.2,0.9)	0.7 (0.3,1.0)	0.8 (0.5,1.0)	0.0 (0.0,10 ⁻²)
σ	0.8 (0.7,0.9)	0.4 (0.3,0.5)	0.4 (0.3,0.5)	0.6 (0.4,0.8)	0.7 (0.6,0.8)
ν	-	1.4 (0.7,2.3)	2.2 (1.4,3.3)	1.9 (1.3,2.8)	-

TABLE 1 Model assessment (WAIC) and parameter posterior summaries: posterior mean and 95% credible interval (CI) for BYM2, BYM2-logCAR, BYM2-Gamma, Congdon and Leroux.

to the neighbourhood structure for the κ 's. In the BYM2-Gamma model, the κ 's are independently and identically distributed, *a priori*, similarly to Congdon's model, and only intervene on the variance of the latent effects. In Congdon's model, the κ 's also have an impact on the conditional means of the latent effects. Regarding the BYM2-logCAR model, the κ 's intervene only on the variance of the latent effects while incorporating the neighbourhood structure in their prior distribution. We believe that these distinct roles and distributions for the mixing parameters explain the differences in the outliers identified after accounting for the socio-development index.

4 | DISCUSSION

In this paper, we propose a disease mapping model that is able to identify areas with potentially outlying disease risks after accounting for the effects of covariates. The proposed model is a scale mixture of the BYM2 model²¹. Two different prior specifications are proposed for the scale mixture components in order to account for potential outliers with respect to the whole region of interest and to consider spatially structured mixture components. Our model allows for a straightforward interpretation of the parameters, that is common to every data application, while accommodating outliers. The parameters' interpretation is eased by the scaling process of the latent spatially structured components¹⁹. For one version of the proposed model, namely the BYM2-Gamma, the focus is only on outliers with respect to the whole region of interest, as decision makers may be interested in determining the areas where an intervention is essential. For the other version of the proposed model, namely the BYM2-logCAR, the potential outliers with respect to the whole region are of interest while incorporating a spatial structure in the mixture components. This parametrisation may help identify clusters of potentially outlying areas.

A simulation study presents the performance of the two versions of the proposed model in comparison with the one by Congdon¹¹, which specifically accommodates local outliers. That is, Congdon¹¹ aims to identify areas that are different from their neighbours. In this simulation study, the neighbourhood structure of Rio de Janeiro is used and the latent effects of some districts are contaminated to control the presence of outliers after accounting for some covariate. The two versions of the proposed model always perform best in terms of WAIC and are able to detect all the contaminated districts. However, the proposed model with scale mixture inspired by Palacios and Steel¹⁰ detects one particular contaminated district only 83% of the time. The model by Congdon¹¹, on the other hand, finds more outliers than are generated, showing more sensitivity to the neighbourhood structure.

The many other simulation studies that are not presented in this paper show that the BYM2-logCAR proposed model is fairly sensitive to the choice of prior mean for the hyperparameter of the scaling mixture components. A smaller prior mean tends to restrict the outliers indicators around 1 while a larger value allows departure from 1. This departure from 1 may be towards 0, which accommodates outliers, or may be towards infinity. Further research might help assigning this prior mean. Finally, in all

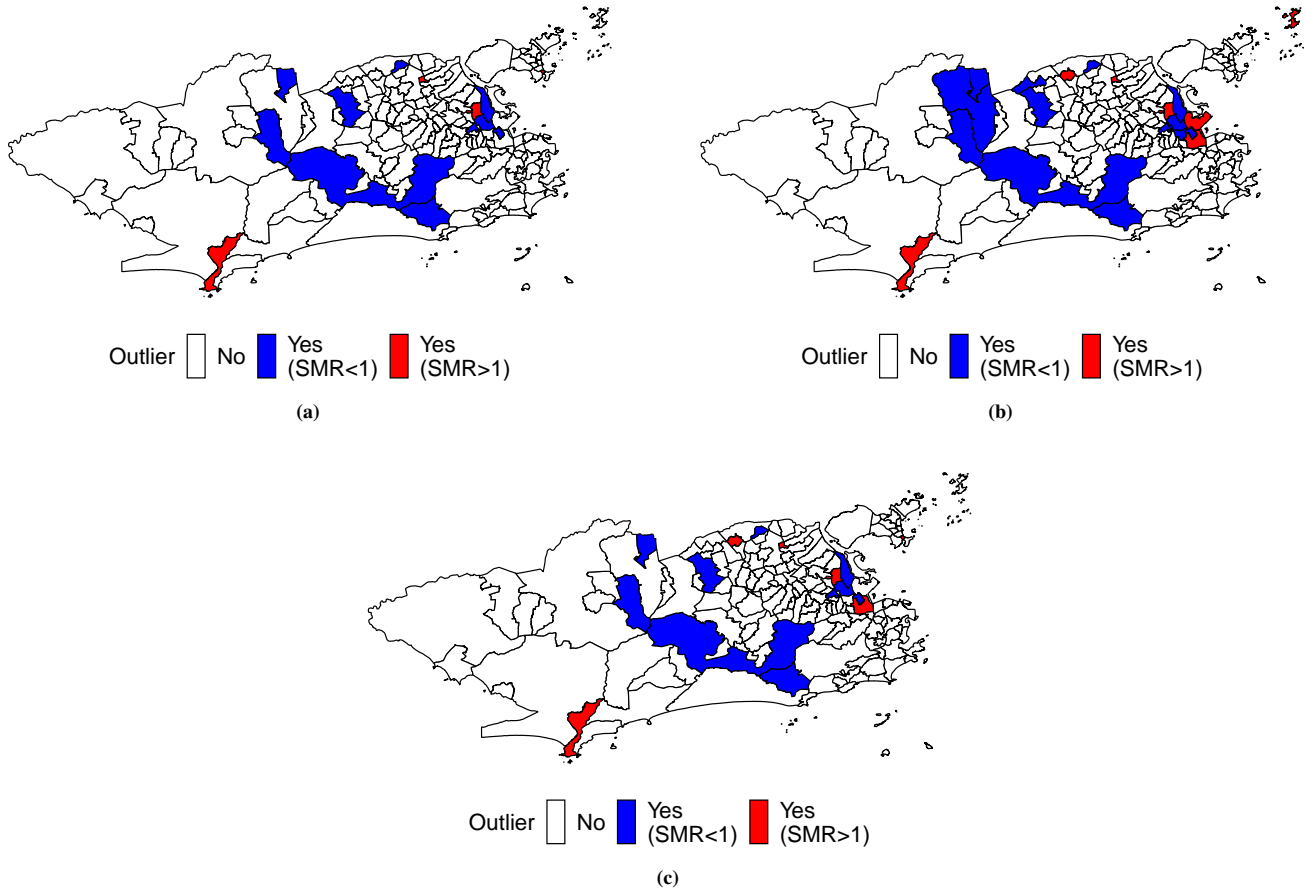


FIGURE 7 Maps of the outliers indicated by $\kappa_u < 1$, where κ_u is the upper bound of the posterior 95% credible interval of κ . The outliers on the lower tail are distinguished from the ones on the upper tail of the SMR distribution. a) BYM2-Gamma model; b) BYM2-logCAR model; c) Congdon's model.

of our simulation studies, the proposed model always performs at least as well as Congdon's, and often better, both in terms of WAIC and of outliers identification.

The cases of Zika that were recorded in Rio de Janeiro during the first 2015-2016 epidemic are analysed using the two parametrisations of the proposed model as well as the model by Congdon¹¹, the BYM2²¹ and the Leroux prior¹⁸. All five models find that there is a fairly strong negative association between the socio-development index and the number of cases, meaning that richer districts have lower disease risks. This finding is consistent with previous studies conducted in Rio de Janeiro, one investigating the first chikungunya epidemic in the city⁸ and another also investigating Zika, but using a different methodological approach³¹. These studies, including ours, indicate that improving sanitary conditions and reducing socio-economic disparities are of paramount importance to fight *Aedes*-borne diseases.

After accounting for the effect of the socio-development index, some neighbourhoods are detected as potential outliers by the proposed models and Congdon's, both in the lower and upper tails of the number of cases' distribution across the districts. By focusing on local outliers, Congdon's model reports a few more potential outliers than the proposed model whose interest lies only in the outlying areas with respect to the whole region of interest, namely the BYM2-Gamma version. Out of the 21 neighbourhoods identified as outliers, irrespective of the model, the proposed models BYM2-logCAR and BYM2-Gamma identified 19 (90.5%) and 14 (66.7%), respectively. Three outlying neighbourhoods did not report any cases (Parque Columbia, Vasco da Gama and Gericinó) and were identified as outliers by the three models.

The detection of outliers with fewer cases than expected can potentially indicate locations with underreporting issues. It is also possible that the neighbourhood of residency is not accurate for some of the cases. It is not uncommon in Rio de Janeiro for a person to report as the neighborhood of residence a neighborhood that actually borders where they live. For example, a

person living in Vasco da Gama may report São Cristóvão as their district. This may be a reason why some neighbourhoods were detected as outliers by the BYM2-logCAR and the Congdon models but not by the BYM2-Gamma. If a given district is accounting for a proportion of the cases that are in fact from the neighbouring areas, this would increase the risk of this district while decreasing the risk of its neighbours. Therefore, the inaccurate information on the district of residency may artificially create outliers. However, this issue may not bias the detection of outliers by the BYM2-Gamma model, because it looks for outliers with respect to the whole study area, and not to their neighbours.

The detection of outliers with more cases than expected after controlling for the socio-development index pinpoints locations that should be further investigated to understand why the elevated risk of Zika in these districts. One possible explanation, discussed above, involves the inaccurate information on the district of residency by a proportion of the cases. However, other underlying characteristics, not included in the models, may be related to this outlying behaviour. Also, it is important to emphasize that some socio-environmental factors that influence the burden and distribution of *Aedes*-borne diseases may be heterogeneous within the districts, our spatial unit of analysis. For example, the same district may have areas with *favelas* (slums) and areas with middle and upper class condominiums. The socio-development index will not capture this intra-district social inequality, and a recent study showed evidence about the presence of socio-economic inequalities in the distribution of dengue, Zika and chikungunya in two Latin American cities³². Another possibility is the presence of large potential breeding sites, such as dumps and vacant lots.

To conclude, we believe our proposed model to be useful to decision makers. First, the parameters' interpretation eases the use of our model regardless of the data spatial structure. This may help decision makers to create a systematic procedure to analyse data with our proposed model in which non informative priors for the parameters could be defined for any spatial structure. Then, the introduction of scaling mixture components improves the recovering of the observed and potentially outlying disease risks, as assessed by the model performance criterion (WAIC). Finally, these mixture components together with high estimated risk ratios help identify all of the potential outlying areas in which interventions may need to be prioritised.

ACKNOWLEDGMENTS

Schmidt and Michal are grateful for the financial support from the Natural Sciences and Engineering Research Council (NSERC) of Canada (Discovery Grant RGPIN-2017-04794) and the IVADO Fundamental Research Project (PRF-2019-6839748021).

DATA AVAILABILITY STATEMENT

The Zika and the population data analysed in this study come from the Brazilian Notifiable Diseases Information System (SINAN - Sistema de Informação de Agravos de Notificação) and the Brazilian Institute of Geography and Statistics (IBGE - Instituto Brasileiro de Geografia e Estatística), respectively, and are publicly available at the Rio de Janeiro Secretariat of Health website (<http://www.rio.rj.gov.br/dlstatic/10112/7079759/4197436/ZIKASE2015.pdf> and <http://www.rio.rj.gov.br/dlstatic/10112/10617973/4260330/ZIKASE2016.pdf>, for 2015 and 2016, respectively). The sociodevelopment index data come from the Instituto Pereira Passos and can be found at www.data.rio.

References

1. Lowe R, Barcellos C, Brasil P, et al. The Zika Virus Epidemic in Brazil: From Discovery to Future Implications. *International Journal of Environmental Research and Public Health* 2018; 15(1): 96. doi: 10.3390/ijerph15010096
2. World Health Organization . Vector-borne diseases. <https://www.who.int/news-room/fact-sheets/detail/vector-borne-diseases>; 2020.
3. Colón-González FJ, Sewe MO, Tompkins AM, et al. Projecting the risk of mosquito-borne diseases in a warmer and more populated world: a multi-model, multi-scenario intercomparison modelling study. *The Lancet Planetary Health* 2021; 5(7): e404–e414. doi: 10.1016/s2542-5196(21)00132-7

4. Freitas LP, Cruz OG, Lowe R, Carvalho MS. Space–time dynamics of a triple epidemic: dengue, chikungunya and Zika clusters in the city of Rio de Janeiro. *Proceedings of the Royal Society B: Biological Sciences* 2019; 286(1912): 20191867. doi: 10.1098/rspb.2019.1867
5. Nogueira RMR, Miagostovich MP, Schatzmayr HG, et al. Dengue in the State of Rio de Janeiro, Brazil, 1986–1998. *Memórias do Instituto Oswaldo Cruz* 1999; 94(3): 297–304. doi: 10.1590/s0074-02761999000300004
6. Honório NA, Nogueira RMR, Codeço CT, et al. Spatial Evaluation and Modeling of Dengue Seroprevalence and Vector Density in Rio de Janeiro, Brazil. *PLoS Neglected Tropical Diseases* 2009; 3(11): e545. doi: 10.1371/journal.pntd.0000545
7. Santos dJPC, Honório NA, Nobre AA. Definition of persistent areas with increased dengue risk by detecting clusters in populations with differing mobility and immunity in Rio de Janeiro, Brazil. *Cadernos de Saúde Pública* 2019; 35(12). doi: 10.1590/0102-311x00248118
8. Freitas LP, Schmidt AM, Cossich W, Cruz OG, Carvalho MS. Spatio-temporal modelling of the first Chikungunya epidemic in an intra-urban setting: The role of socioeconomic status, environment and temperature. *PLOS Neglected Tropical Diseases* 2021; 15(6): e0009537. doi: 10.1371/journal.pntd.0009537
9. Prefeitura do Rio de Janeiro . Índice de Desenvolvimento Social (IDS) por Áreas de Planejamento (AP), Regiões de Planejamento (RP), Regiões Administrativas (RA), Bairros e Favelas do Município do Rio de Janeiro - 2010. <http://www.data.rio/datasets/fa85ddc76a524380ad7fc60e3006ee97>; 2018.
10. Palacios MB, Steel MFJ. Non-Gaussian Bayesian geostatistical modeling. *Journal of the American Statistical Association* 2006; 101(474): 604–618.
11. Congdon P. Representing spatial dependence and spatial discontinuity in ecological epidemiology: a scale mixture approach. *Stochastic Environmental Research and Risk Assessment* 2017; 31(2): 291–304.
12. Dean N, Dong G, Piekut A, Pryce G. Frontiers in residential segregation: Understanding neighbourhood boundaries and their impacts. *Tijdschrift voor economische en sociale geografie* 2019; 110(3): 271–288.
13. Besag J. Spatial interaction and the statistical analysis of lattice systems. *Journal of the Royal Statistical Society: Series B (Methodological)* 1974; 36(2): 192–225.
14. Banerjee S, Carlin BP, Gelfand AE. *Hierarchical modeling and analysis for spatial data*. CRC press . 2014.
15. Breslow N, Leroux B, Platt R. Approximate hierarchical modelling of discrete data in epidemiology. *Statistical Methods in Medical Research* 1998; 7(1): 49–62.
16. Besag J, York J, Mollié A. Bayesian image restoration, with two applications in spatial statistics. *Annals of the institute of statistical mathematics* 1991; 43(1): 1–20.
17. MacNab YC. On Gaussian Markov random fields and Bayesian disease mapping. *Statistical Methods in Medical Research* 2011; 20(1): 49–68.
18. Leroux BG, Lei X, Breslow N. Estimation of disease rates in small areas: a new mixed model for spatial dependence. In: Springer. 1999 (pp. 179–191).
19. Sørbye SH, Rue H. Scaling intrinsic Gaussian Markov random field priors in spatial modelling. *Spatial Statistics* 2014; 8: 39–51.
20. Best NG, Arnold RA, Thomas A, Waller LA, Conlon EM. Bayesian models for spatially correlated disease and exposure data. 1999; 6: 131–156.
21. Riebler A, Sørbye SH, Simpson D, Rue H. An intuitive Bayesian spatial model for disease mapping that accounts for scaling. *Statistical methods in medical research* 2016; 25(4): 1145–1165.
22. Yan J. Spatial stochastic volatility for lattice data. *Journal of agricultural, biological, and environmental statistics* 2007; 12(1): 25–40.

23. Rue H, Held L. *Gaussian Markov random fields: theory and applications*. CRC press . 2005.
24. Gelman A, Carlin JB, Stern HS, Dunson DB, Vehtari A, Rubin DB. *Bayesian data analysis*. CRC press . 2004.
25. Stan Development Team . RStan: the R interface to Stan. 2020. R package version 2.21.2.
26. Morris M, Wheeler-Martin K, Simpson D, Mooney SJ, Gelman A, DiMaggio C. Bayesian hierarchical spatial models: Implementing the Besag York Mollié model in stan. *Spatial and spatio-temporal epidemiology* 2019; 31: 100301.
27. Rue H, Martino S, Chopin N. Approximate Bayesian inference for latent Gaussian models by using integrated nested Laplace approximations. *Journal of the royal statistical society: Series b (statistical methodology)* 2009; 71(2): 319–392.
28. Gelman A, Rubin DB, others . Inference from iterative simulation using multiple sequences. *Statistical science* 1992; 7(4): 457–472.
29. Vehtari A, Gelman A, Simpson D, Carpenter B, Bürkner PC. Rank-Normalization, Folding, and Localization: An Improved \hat{R} for Assessing Convergence of MCMC. *Bayesian Analysis* 2021: 1–38. . doi: 10.1214/20-BA1221
30. Watanabe S, Opper M. Asymptotic equivalence of Bayes cross validation and widely applicable information criterion in singular learning theory.. *Journal of machine learning research* 2010; 11(12).
31. Raymundo CE, Andrade Medronho dR. Association between socio-environmental factors, coverage by family health teams, and rainfall in the spatial distribution of Zika virus infection in the city of Rio de Janeiro, Brazil, in 2015 and 2016. *BMC Public Health* 2021; 21(1). doi: 10.1186/s12889-021-11249-y
32. Carabali M, Harper S, Neto ASL, et al. Spatiotemporal distribution and socioeconomic disparities of dengue, chikungunya and Zika in two Latin American cities from 2007 to 2017. *Tropical Medicine & International Health* 2020; 26(3): 301–315. doi: 10.1111/tmi.13530

How to cite this article: Michal V., Freitas L.P., Schmidt A.M. (2021), A Bayesian hierarchical model for disease mapping that accounts for scaling and heavy-tailed latent effects, *Statistics in Medicine*, 20XX;XX:XX–XX.

APPENDIX

A STAN CODE FOR THE PROPOSED MODEL

The stan code used to fit the proposed BYM2-Gamma model in the simulation studies (section 3.1, Appendix C, Appendix E) and in the analysis of the Zika epidemic in Rio de Janeiro (section 3.2) is presented below.

Listing 1: Stan code for the BYM2-Gamma proposed model

```

1 data {
2   int<lower=1> N;
3   int<lower=1> N_edges;
4   int<lower=1> p; // General case where there are p covariates
5   matrix[N,p] X;
6   int<lower=1, upper=N> node1[N_edges]; // vectors of neighbourhood
7   int<lower=1, upper=N> node2[N_edges]; // structure
8   int<lower=0> y[N]; // Zika counts
9   vector<lower=0>[N] log_E; // offset
10  real<lower=0> scaling_factor; // to scale the variance of the latent effects
11 }
12
13 parameters {
```

```

14  real beta0; // intercept
15  vector[p] beta;
16  real<lower=0> sigma; // marginal standard deviation
17  real<lower=0, upper=1> lambda; // mixing parameter
18  vector[N] theta; // unstructured components
19  vector[N] s; // spatially structured components
20  vector<lower=0>[N] kappa; // outlier indicator
21  real<lower=0> nu;
22  }
23
24  transformed parameters {
25    vector[N] convolved_re; // complete latent effect
26    for(i in 1:N){ convolved_re[i] = sqrt(1 - lambda) * theta[i] + sqrt(lambda/scaling_factor) * s[i]; }
27  }
28
29  model {
30    for(i in 1:N)
31      y[i] ~ poisson_log(log_E[i] + beta0 + X[i,]*beta + convolved_re[i] * (sigma/sqrt(kappa[i])) );
32
33    target += -0.5 * dot_self(s[node1] - s[node2]); // Prior for the spatially structured components
34    sum(s) ~ normal(0, 0.001 * N); // Soft sum-to-zero constraint to be able to have an intercept
35
36    for(j in 1:p){ beta[j] ~ normal(0.0, 10.0); }
37
38    beta0 ~ normal(0.0, 10.0);
39    theta ~ normal(0.0, 1.0);
40    sigma ~ normal(0.0, 1.0);
41    lambda ~ uniform(0.0, 1.0);
42    kappa ~ gamma(nu/2.0, nu/2.0);
43    nu ~ exponential(1.0/4.0);
44  }
45
46  generated quantities {
47    vector[N] mu_log;
48    vector[N] lik;
49    for(i in 1:N){
50      mu_log[i]=log_E[i] + beta0 + X[i,]*beta + sigma*convolved_re[i]/sqrt(kappa[i]);
51      lik[i] = exp(poisson_log_lpmf(y[i] | mu_log[i])); // likelihood to compute the WAIC
52    }
53  }

```

B ADDITIONAL RESULTS FROM THE ZIKA DATA ANALYSIS

This section shows the maps of the posterior means for the latent effects obtained from fitting the BYM2, the proposed BYM2-Gamma, the proposed BYM2-logCAR, Congdon's and the Leroux models in Figure B1. Additionally, in Table B1, this section provides the posterior means and posterior 95% credible intervals for the scale mixture components, κ , included in the proposed BYM2-Gamma and BYM2-logCAR models as well as in Congdon's prior.

District	BYM2-Gamma	BYM2-logCAR	Congdon
----------	------------	-------------	---------

Saude	1.4 (0.11,4.37)	4.9 (0.12,30)	1.1 (0.07,3.82)
Gamboa	1.5 (0.15,4.58)	2.4 (0.12,11.37)	1.2 (0.09,3.84)
Santo Cristo	0.5 (0.05,1.34)	0.4 (0.08,1.22)	0.5 (0.03,1.48)
Caju	0.9 (0.06,2.59)	0.2 (0.03,0.65)	0.7 (0.04,2.69)
Centro	1.3 (0.14,3.48)	1.0 (0.17,3.16)	1.5 (0.12,3.77)
Catumbi	0.8 (0.08,2.14)	0.7 (0.09,2.19)	1.1 (0.09,2.99)
Rio Comprido	0.9 (0.09,2.63)	0.8 (0.11,2.33)	1.8 (0.16,4.22)
Cidade Nova	1.5 (0.19,4.61)	1.0 (0.13,3.45)	1.6 (0.10,4.69)
Estacio	0.9 (0.09,2.51)	0.8 (0.09,2.57)	1.1 (0.08,3.06)
Sao Cristovao	0.4 (0.03,1.19)	0.2 (0.04,0.69)	0.3 (0.01,0.97)
Mangueira	0.8 (0.05,2.44)	0.4 (0.04,1.47)	0.8 (0.04,3.08)
Benfica	1.1 (0.08,3.50)	0.2 (0.04,0.72)	1.0 (0.05,3.84)
Paqueta	0.3 (0.03,1.04)	0.3 (0.01,0.94)	0.4 (0.02,1.16)
Santa Teresa	0.6 (0.06,1.77)	0.8 (0.20,1.94)	0.6 (0.03,1.64)
Flamengo	1.1 (0.07,3.35)	1.7 (0.14,6.80)	0.9 (0.05,3.16)
Gloria	1.3 (0.10,3.84)	1.7 (0.15,6.39)	1.2 (0.08,3.67)
Laranjeiras	1.2 (0.09,3.73)	1.6 (0.16,6.11)	1.1 (0.07,3.68)
Catete	1.4 (0.12,4.29)	2.2 (0.17,8.46)	1.3 (0.09,4.20)
Cosme Velho	1.1 (0.06,3.66)	1.7 (0.10,7.78)	1.0 (0.05,3.45)
Botafogo	0.9 (0.07,2.81)	1.2 (0.25,3.33)	0.6 (0.03,2.05)
Humaita	1.2 (0.10,3.68)	1.3 (0.21,4.10)	1.2 (0.07,3.82)
Urca	1.1 (0.09,3.28)	1.8 (0.13,8.16)	1.1 (0.08,3.36)
Leme	1.2 (0.11,3.66)	2.1 (0.18,8.96)	1.4 (0.12,4.28)
Copacabana	1.5 (0.12,4.40)	2.1 (0.25,7.69)	1.5 (0.11,4.48)
Ipanema	1.4 (0.11,4.66)	2.4 (0.13,11.67)	1.5 (0.08,4.89)
Leblon	0.5 (0.03,1.63)	0.7 (0.07,2.25)	0.4 (0.03,1.60)
Lagoa	1.2 (0.08,3.89)	1.4 (0.19,4.80)	1.2 (0.06,4.07)
Jardim Botânico	1.4 (0.08,4.28)	1.7 (0.15,7.09)	1.3 (0.08,4.39)
Gavea	1.0 (0.07,3.25)	0.9 (0.12,2.94)	0.9 (0.05,3.36)
Vidigal	0.9 (0.07,3.02)	0.8 (0.07,2.81)	0.7 (0.03,2.39)
Sao Conrado	1.1 (0.07,3.79)	0.7 (0.09,2.14)	1.0 (0.04,3.65)
Praca da Bandeira	1.2 (0.11,3.40)	0.7 (0.11,2.02)	1.4 (0.11,4.14)
Tijuca	1.0 (0.09,3.02)	0.8 (0.15,2.34)	0.8 (0.06,2.71)
Alto da Boa Vista	1.2 (0.10,3.80)	0.8 (0.16,2.10)	1.0 (0.04,3.25)
Maracana	1.3 (0.10,4.18)	0.7 (0.08,2.37)	1.2 (0.06,4.13)
Vila Isabel	1.3 (0.10,3.99)	0.7 (0.15,2.04)	0.8 (0.04,2.68)
Andaraí	1.0 (0.07,3.29)	1.1 (0.08,4.11)	1.0 (0.05,3.71)
Grajau	1.5 (0.12,4.54)	0.9 (0.14,2.87)	1.3 (0.08,4.19)
Manguinhos	0.3 (0.01,0.88)	0.2 (0.04,0.60)	0.2 (0.01,0.82)
Bonsucesso	0.3 (0.01,0.90)	0.2 (0.03,0.65)	0.2 (0.01,0.58)
Ramos	1.1 (0.10,3.39)	0.5 (0.04,1.82)	0.8 (0.04,2.95)
Olaria	0.8 (0.06,2.50)	0.5 (0.07,1.48)	0.7 (0.04,2.37)
Penha	1.4 (0.12,4.38)	0.7 (0.08,2.61)	1.2 (0.07,4.25)
Penha Circular	0.6 (0.06,1.88)	0.5 (0.09,1.41)	0.5 (0.03,1.77)
Bras de Pina	1.0 (0.08,3.10)	0.6 (0.08,1.99)	0.8 (0.04,2.58)
Cordovil	1.5 (0.12,4.36)	0.7 (0.08,2.60)	1.4 (0.08,4.70)
Parada de Lucas	1.0 (0.08,3.23)	0.6 (0.06,1.96)	1.0 (0.06,3.32)
Vigário Geral	0.6 (0.04,1.70)	0.4 (0.04,1.42)	0.6 (0.04,2.13)
Jardim America	1.5 (0.10,4.77)	0.5 (0.05,2.26)	1.5 (0.09,4.94)
Higienópolis	1.2 (0.08,3.60)	0.6 (0.09,2.12)	1.2 (0.07,3.99)
Jacare	0.9 (0.07,2.83)	0.6 (0.10,1.74)	1.4 (0.10,3.85)

Maria da Graca	1.2 (0.09,3.95)	0.6 (0.07,2.05)	1.5 (0.11,4.71)
Del Castilho	1.4 (0.11,4.55)	1.2 (0.11,5.04)	1.2 (0.07,4.20)
Inhauma	1.5 (0.12,4.59)	1.1 (0.15,3.56)	1.4 (0.08,4.21)
Engenho da Rainha	1.4 (0.12,4.44)	0.8 (0.14,2.43)	1.1 (0.06,3.70)
Tomas Coelho	0.9 (0.07,2.91)	0.9 (0.14,2.64)	1.1 (0.07,3.45)
Sao Francisco Xavier	0.6 (0.05,1.78)	0.4 (0.05,1.28)	0.3 (0.01,1.12)
Rocha	1.0 (0.09,3.04)	0.5 (0.06,1.52)	0.9 (0.06,3.10)
Riachuelo	1.3 (0.11,3.74)	0.9 (0.09,3.27)	1.6 (0.11,4.62)
Sampaio	0.8 (0.07,2.40)	0.7 (0.09,2.48)	1.2 (0.11,3.08)
Engenho Novo	0.9 (0.08,2.80)	0.7 (0.14,2.03)	1.1 (0.07,2.92)
Lins de Vasconcelos	1.5 (0.12,4.61)	1.1 (0.14,3.81)	1.5 (0.11,5.06)
Meier	0.7 (0.05,2.22)	0.7 (0.11,2.05)	0.5 (0.03,1.71)
Todos os Santos	1.0 (0.07,3.23)	1.0 (0.09,3.49)	0.8 (0.04,2.80)
Cachambi	1.4 (0.09,4.39)	0.8 (0.15,2.17)	1.2 (0.07,3.80)
Engenho de Dentro	1.4 (0.11,4.29)	1.0 (0.23,3.06)	1.3 (0.07,3.92)
Agua Santa	1.3 (0.09,4.13)	1.1 (0.17,3.84)	1.2 (0.06,3.88)
Encantado	1.4 (0.09,4.64)	2.2 (0.19,9.33)	1.3 (0.07,4.24)
Piedade	1.4 (0.12,4.20)	1.3 (0.23,3.79)	1.3 (0.08,3.98)
Abolicao	1.2 (0.08,3.77)	1.7 (0.18,6.52)	1.3 (0.08,3.95)
Pilares	1.2 (0.12,3.78)	1.2 (0.18,4.06)	1.3 (0.10,3.78)
Vila Kosmos	0.5 (0.04,1.53)	0.5 (0.08,1.53)	0.6 (0.03,2.22)
Vicente de Carvalho	0.8 (0.05,2.53)	0.7 (0.11,2.08)	1.3 (0.08,4.16)
Vila da Penha	1.2 (0.08,3.99)	0.7 (0.09,2.56)	0.8 (0.03,2.93)
Vista Alegre	0.2 (0.01,0.69)	0.3 (0.04,0.76)	0.2 (0.01,0.55)
Iraja	0.9 (0.05,2.83)	0.5 (0.12,1.13)	0.4 (0.02,1.38)
Colegio	1.4 (0.13,4.31)	1.3 (0.08,6.12)	1.7 (0.10,5.31)
Campinho	1.4 (0.10,4.38)	1.3 (0.17,4.72)	1.2 (0.08,3.98)
Quintino Bocaiuva	0.8 (0.06,2.65)	0.9 (0.16,2.49)	0.8 (0.04,2.31)
Cavalcanti	1.1 (0.10,3.44)	1.0 (0.18,2.98)	1.5 (0.11,4.43)
Engenheiro Leal	0.7 (0.05,2.46)	0.8 (0.08,3.12)	1.0 (0.05,3.00)
Cascadura	1.5 (0.11,4.49)	1.2 (0.17,4.20)	1.3 (0.08,4.31)
Madureira	1.2 (0.11,3.67)	1.0 (0.17,3.16)	1.6 (0.12,4.53)
Vaz Lobo	0.9 (0.07,2.68)	0.8 (0.11,2.55)	0.9 (0.06,3.25)
Turiacu	1.5 (0.13,4.53)	1.1 (0.13,4.18)	1.3 (0.08,4.17)
Rocha Miranda	0.9 (0.06,2.85)	0.8 (0.16,2.17)	0.6 (0.04,1.91)
Honorio Gurgel	1.4 (0.11,4.06)	1.1 (0.16,3.70)	1.4 (0.09,4.26)
Osvaldo Cruz	0.7 (0.05,2.09)	0.8 (0.12,2.28)	0.6 (0.03,1.82)
Bento Ribeiro	1.4 (0.12,4.18)	1.3 (0.19,4.25)	1.3 (0.10,4.13)
Marechal Hermes	1.4 (0.10,3.97)	1.1 (0.17,3.59)	1.4 (0.10,4.19)
Ribeira	1.5 (0.11,4.47)	3.3 (0.02,22.45)	1.6 (0.09,5.80)
Zumbi	0.2 (0.01,0.91)	0.3 (0.04,1.04)	0.2 (0.01,0.59)
Cacuia	1.2 (0.08,3.71)	1.1 (0.12,3.78)	1.2 (0.07,3.81)
Pitangueiras	0.9 (0.07,2.82)	0.7 (0.05,2.74)	1.2 (0.06,3.57)
Praia da Bandeira	0.9 (0.06,2.92)	0.9 (0.06,3.85)	1.0 (0.05,3.14)
Cocota	1.1 (0.08,3.74)	1.4 (0.12,5.38)	0.6 (0.03,2.61)
Bancarios	1.4 (0.12,4.22)	2.3 (0.10,10.38)	1.5 (0.09,4.32)
Freguesia (Ilha)	1.0 (0.08,3.18)	1.6 (0.04,6.78)	1.0 (0.06,2.88)
Jardim Guanabara	1.4 (0.10,4.20)	1.9 (0.16,8.57)	1.3 (0.06,4.12)
Jardim Carioca	1.4 (0.10,4.27)	1.8 (0.20,7.86)	1.4 (0.09,4.40)
Taua	0.7 (0.04,2.16)	1.0 (0.11,3.42)	0.5 (0.03,1.60)
Monero	1.4 (0.11,4.27)	2.8 (0.15,11.91)	1.4 (0.07,4.30)

Portuguesa	1.1 (0.09,3.59)	1.8 (0.16,7.16)	1.0 (0.05,3.23)
Galeao	1.4 (0.10,4.37)	0.7 (0.10,2.50)	1.2 (0.07,3.90)
Cidade Universitaria	1.2 (0.07,3.82)	0.5 (0.03,2.14)	1.2 (0.06,4.55)
Guadalupe	1.4 (0.13,4.18)	0.8 (0.12,2.67)	1.4 (0.09,4.29)
Anchieta	1.2 (0.10,3.70)	0.6 (0.07,2.01)	1.7 (0.10,4.85)
Parque Anchieta	0.3 (0.03,1.08)	0.3 (0.04,0.82)	0.4 (0.02,1.36)
Ricardo de Albuquerque	0.9 (0.08,2.70)	0.6 (0.07,1.87)	1.1 (0.08,3.40)
Coelho Neto	1.4 (0.12,4.78)	0.6 (0.10,2.01)	1.4 (0.10,4.65)
Acari	1.4 (0.11,3.97)	0.6 (0.05,2.39)	1.4 (0.07,4.53)
Barros Filho	0.8 (0.06,2.50)	0.6 (0.09,1.88)	0.7 (0.04,2.33)
Costa Barros	0.3 (0.02,1.02)	0.3 (0.04,0.92)	0.2 (0.01,0.58)
Pavuna	1.3 (0.12,4.02)	0.5 (0.08,1.47)	1.3 (0.09,4.26)
Jacarepagua	0.2 (0.01,0.69)	0.4 (0.10,0.79)	0.1 (0.00,0.20)
Anil	0.5 (0.05,1.66)	0.4 (0.04,1.33)	0.5 (0.02,2.16)
Gardenia Azul	0.6 (0.04,1.85)	0.4 (0.06,1.35)	0.5 (0.02,2.15)
Cidade de Deus	1.0 (0.06,3.20)	0.7 (0.09,2.42)	0.7 (0.03,2.84)
Curicica	0.5 (0.03,1.63)	0.4 (0.03,1.34)	1.0 (0.05,3.87)
Freguesia (Jacarepagua)	1.3 (0.08,4.03)	0.8 (0.15,2.38)	0.7 (0.04,2.77)
Pechincha	1.2 (0.09,3.48)	0.9 (0.11,3.47)	1.1 (0.06,3.61)
Taquara	0.6 (0.04,1.81)	0.5 (0.09,1.39)	1.0 (0.05,3.22)
Tanque	1.4 (0.12,4.27)	1.0 (0.16,3.03)	2.1 (0.15,6.09)
Praca Seca	0.7 (0.06,2.30)	0.8 (0.14,2.46)	0.8 (0.04,2.50)
Vila Valqueire	1.4 (0.11,4.52)	1.1 (0.16,3.65)	1.4 (0.08,4.55)
Joa	1.0 (0.04,3.65)	1.3 (0.04,8.09)	1.0 (0.04,3.56)
Itanhanga	0.2 (0.01,0.66)	0.3 (0.04,0.72)	0.2 (0.01,0.72)
Barra da Tijuca	1.4 (0.11,4.34)	0.7 (0.09,2.21)	1.4 (0.09,5.16)
Camorim	0.5 (0.03,1.59)	0.4 (0.06,1.30)	0.3 (0.02,1.15)
Vargem Pequena	1.4 (0.10,4.28)	1.1 (0.06,5.08)	1.3 (0.06,4.51)
Vargem Grande	1.2 (0.10,3.89)	0.5 (0.10,1.66)	1.2 (0.08,3.87)
Recreio dos Bandeirantes	1.4 (0.11,4.36)	0.7 (0.07,2.49)	1.4 (0.08,4.64)
Grumari	0.9 (0.03,3.58)	0.7 (0.02,4.39)	0.9 (0.03,3.53)
Deodoro	1.4 (0.11,4.38)	1.0 (0.10,3.59)	1.4 (0.10,4.29)
Vila Militar	0.2 (0.01,0.58)	0.2 (0.05,0.67)	0.1 (0.00,0.37)
Campo dos Afonsos	1.2 (0.09,3.62)	0.9 (0.11,3.60)	1.1 (0.05,3.72)
Jardim Sulacap	0.8 (0.06,2.58)	0.6 (0.10,1.72)	0.9 (0.05,2.85)
Magalhaes Bastos	1.3 (0.09,3.93)	0.9 (0.04,4.45)	1.2 (0.07,3.97)
Realengo	1.5 (0.12,4.63)	0.5 (0.08,1.34)	1.3 (0.06,4.66)
Padre Miguel	0.9 (0.08,2.70)	0.5 (0.03,2.15)	1.7 (0.07,5.62)
Bangu	0.5 (0.04,1.41)	0.3 (0.04,0.85)	0.8 (0.05,2.62)
Senador Camara	0.3 (0.02,0.91)	0.3 (0.06,0.89)	0.2 (0.01,0.74)
Santissimo	1.2 (0.09,3.86)	0.7 (0.07,2.60)	1.5 (0.09,4.78)
Campo Grande	1.4 (0.12,4.19)	0.7 (0.13,1.90)	1.4 (0.08,4.40)
Senador Vasconcelos	1.2 (0.10,3.62)	0.8 (0.06,3.66)	0.8 (0.05,2.89)
Inhoaiba	1.4 (0.11,4.48)	1.8 (0.11,9.18)	1.3 (0.08,4.54)
Cosmos	0.9 (0.05,3)	0.9 (0.11,2.88)	0.6 (0.03,1.90)
Paciencia	1.2 (0.10,3.55)	1.1 (0.09,5.07)	0.8 (0.05,2.49)
Santa Cruz	1.5 (0.12,4.59)	1.4 (0.10,6.01)	1.2 (0.07,4.17)
Sepetiba	0.7 (0.06,2.06)	0.6 (0.05,2.03)	0.7 (0.04,2.35)
Guaratiba	1.2 (0.08,3.58)	0.6 (0.11,1.97)	1.7 (0.13,4.56)
Barra de Guaratiba	0.2 (0.01,0.64)	0.2 (0.03,0.65)	0.2 (0.01,0.57)
Pedra de Guaratiba	0.4 (0.03,1.26)	0.3 (0.02,1.09)	0.6 (0.03,2.06)

Rocinha	0.9 (0.07,2.76)	0.7 (0.06,2.78)	0.7 (0.03,2.53)
Jacarezinho	0.1 (0.01,0.35)	0.2 (0.03,0.46)	0.1 (0.00,0.26)
Complexo do Alemão	1.1 (0.08,3.38)	0.6 (0.09,1.97)	1.0 (0.05,3.20)
Mare	0.1 (0.00,0.16)	0.1 (0.03,0.30)	0.0 (0.00,0.09)
Parque Columbia	0.0 (0.00,0.08)	0.1 (0.01,0.23)	0.0 (0.00,0.05)
Vasco da Gama	0.0 (0.00,0.06)	0.0 (0.00,0.11)	0.0 (0.00,0.05)
Gericino	0.0 (0.00,0.21)	0.0 (0.00,0.15)	0.1 (0.00,0.78)

TABLE B1 Posterior summaries (mean and 95% credible interval) of the scale mixture components, the κ 's, in each district for the proposed BYM2-Gamma and BYM2-logCAR models and Congdon's

C SIMULATION STUDY: GENERATING DATA FROM THE PROPOSED BYM2-GAMMA MODEL

To assess the proposed BYM2-Gamma model's ability to recover the truth, a simulation study is conducted wherein data are generated from the proposed BYM2-Gamma model. Again, the $n = 160$ districts of Rio de Janeiro and their neighbourhood structure are used. The latent effects' unstructured and scaled spatially structured components are generated once:

$$\boldsymbol{\theta} \sim \mathcal{N}(\mathbf{0}, \mathbf{I}), \quad \text{and} \quad \mathbf{u}^* \sim \mathcal{N}(\mathbf{0}, \mathbf{Q}_*^-),$$

where $\mathbf{Q}_* = h(\mathbf{D} - \mathbf{W})$, with h , the scaling factor, entirely defined by the spatial structure of Rio de Janeiro. An algorithm to generate from the CAR prior is presented in Chapter 2 of Rue and Held²³. The outlier indicators, $\boldsymbol{\kappa}$, are independently generated once from a $\text{Gamma}(\nu/2, \nu/2)$, with an arbitrary $\nu = 4$ to allow for fairly heavy tails. The latent effects are then computed as

$$b_i = \left[\sqrt{1 - \lambda} \theta_i + \sqrt{\lambda} u_i^* \right] \times \sigma / \sqrt{\kappa_i}, \quad i = 1, \dots, n,$$

where $\lambda = 0.8$ and $\sigma = 0.3$. Finally, 100 replicates of populations of size $n = 160$ are generated from the Poisson model

$$Y_i \sim \mathcal{P} \left(E_i \exp [\beta_0 + b_i] \right),$$

with $\beta_0 = -0.1$ and the offsets, $[E_1, \dots, E_n]^\top$, taken from the analysis of the Zika counts. The proposed BYM2-Gamma model and Congdon's are both fitted on the 100 replicated datasets using the same inference procedure as in section 3.1.

Figure C2 shows that the WAIC is able to always choose the model that generated the data, namely the BYM2-Gamma model. This simulation study is specifically conducted to assess whether the proposed BYM2-Gamma model is able to estimate the true values of the generated parameters. Figure C3 presents the posterior summaries obtained from the BYM2-Gamma model across the 100 replicates for the intercept, β_0 , the mixing parameter, λ , the hyperparameter, ν , and the overall standard deviation, σ . For β_0 and ν , the BYM2-Gamma model is able to recover the true values. Regarding λ and σ , the BYM2-Gamma model tends to underestimate these parameters on average but still recovers the truth in the posterior 95% credible intervals. The interest lies particularly on the main parameters of the model, such as the outlier indicators, $\boldsymbol{\kappa}$. Figure C4 shows the estimated densities from the true κ 's (bold line) along with the ones from the first 500 MCMC iterations (gray lines) for three different replicated datasets, namely the 1st, 50th and 100th simulations. The proposed BYM2-Gamma model seems to recover the true distribution of the κ 's. Regarding the complete latent effects, \mathbf{b} , the estimated densities are again displayed in Figure C5. The BYM2-Gamma model estimates accurately the distribution of the latent effects.

D SIMULATION STUDY: GENERATING DATA FROM THE PROPOSED BYM2-LOGCAR MODEL

We now assess the proposed BYM2-logCAR model's ability to recover the truth. Similar to Appendix C, a simulation study is conducted wherein data are generated from the proposed BYM2-logCAR model using the $n = 160$ districts of Rio de Janeiro. The unstructured and spatially structured components, $\boldsymbol{\theta}$ and \mathbf{u}^* respectively, are independently generated once, like in Appendix C. The scaling mixture components, $\boldsymbol{\kappa}$, are generated once using the spatial structure as follows:

$$\mathbf{z} \sim \mathcal{N}(\mathbf{0}, \mathbf{Q}_*^-) \quad \text{and} \quad \kappa_i = \exp \left(-\frac{\nu_\kappa}{2} + \sqrt{\nu_\kappa} z_i \right), \quad i = 1, \dots, n,$$

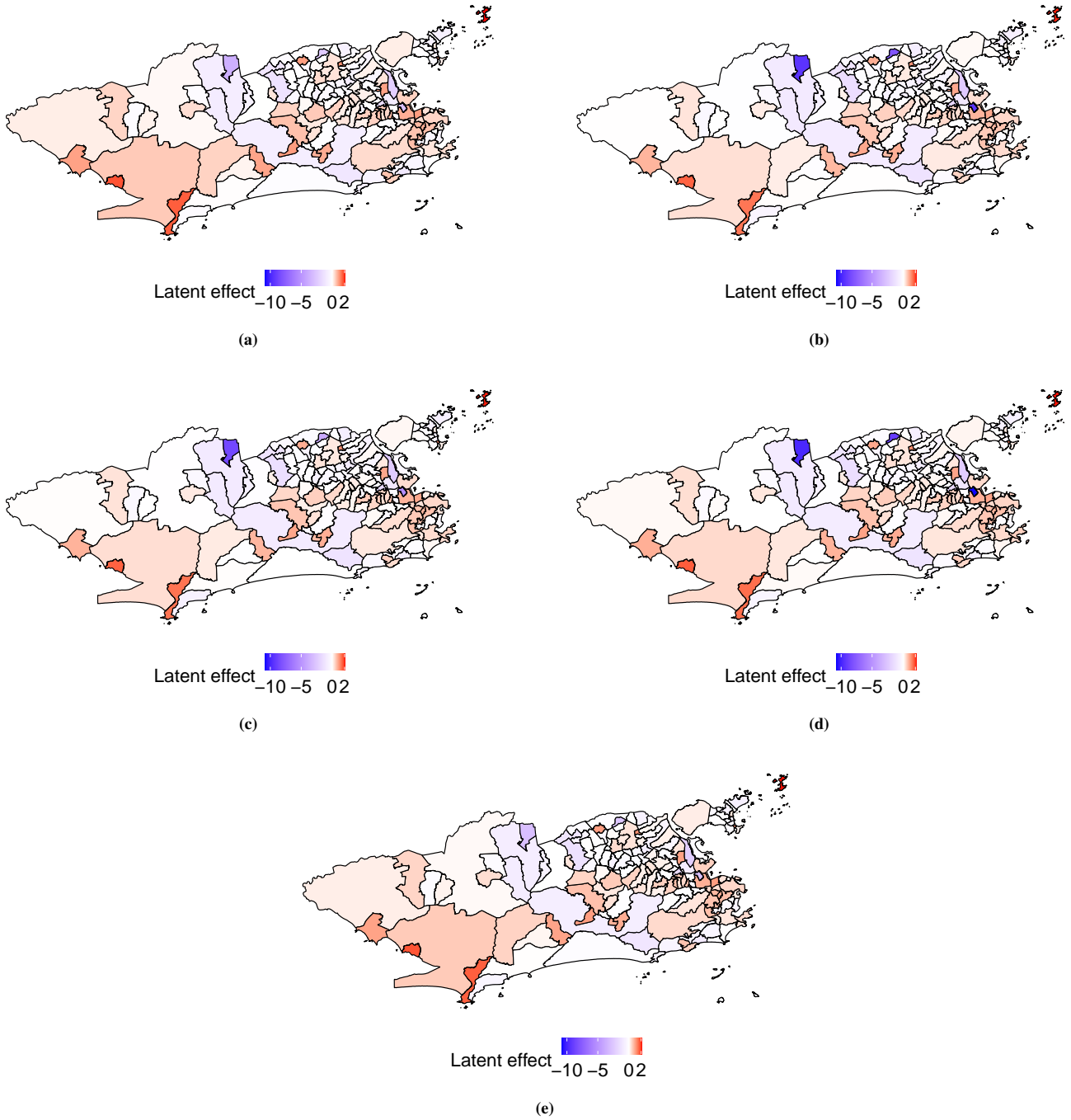


FIGURE B1 Maps of the latent effects' posterior means. a) BYM2 model; b) BYM2-Gamma model; c) BYM2-logCAR model; d) Congdon's prior; e) Leroux prior.

with an arbitrary $v_\kappa = 0.3$ to allow the κ 's to depart from 1. Like in Appendix C, the latent effects are then computed as $b_i = \left[\sqrt{1 - \lambda\theta_i} + \sqrt{\lambda}u_i^* \right] \times \sigma / \sqrt{\kappa_i}$, $i = 1, \dots, n$, where $\lambda = 0.8$ and $\sigma = 0.3$. Finally, 100 replicates of populations of size $n = 160$ are generated from the Poisson model, $Y_i \sim \mathcal{P}(E_i \exp[\beta_0 + b_i])$, with $\beta_0 = -0.1$ and the offsets, $[E_1, \dots, E_n]^\top$, taken from the analysis of the Zika counts. The proposed BYM2-logCAR model and Congdon's are both fitted on the 100 replicated datasets using the same inference procedure as in section 3.1.

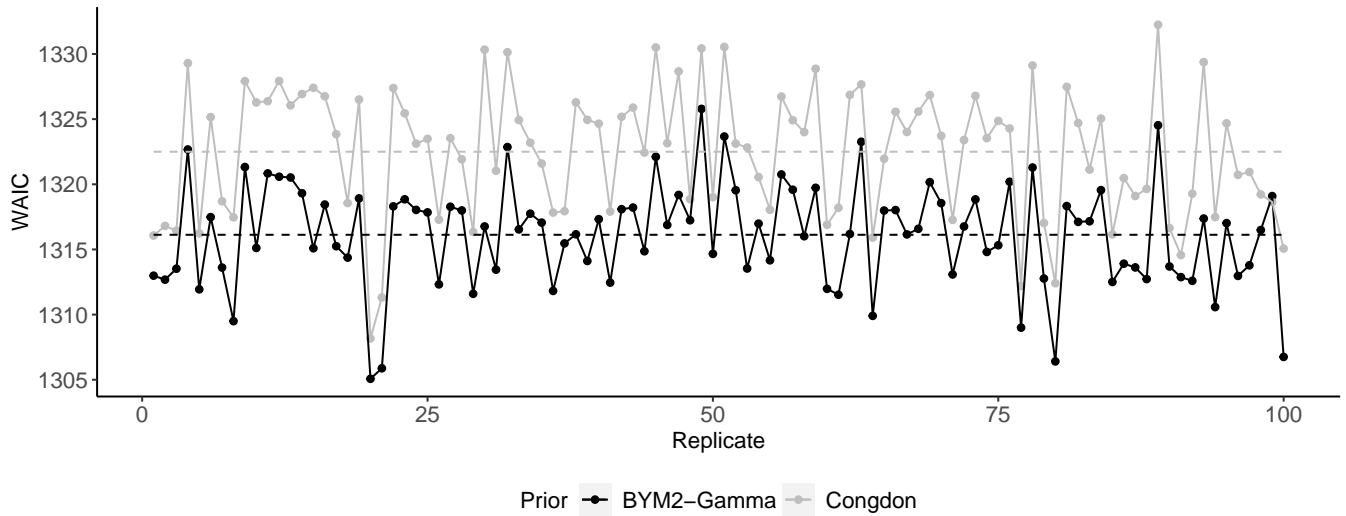


FIGURE C2 WAIC across the 100 replicates for the proposed BYM2-Gamma model and Congdon's regarding the simulated data from the proposed BYM2-Gamma model. Dashed lines: mean WAIC for each model

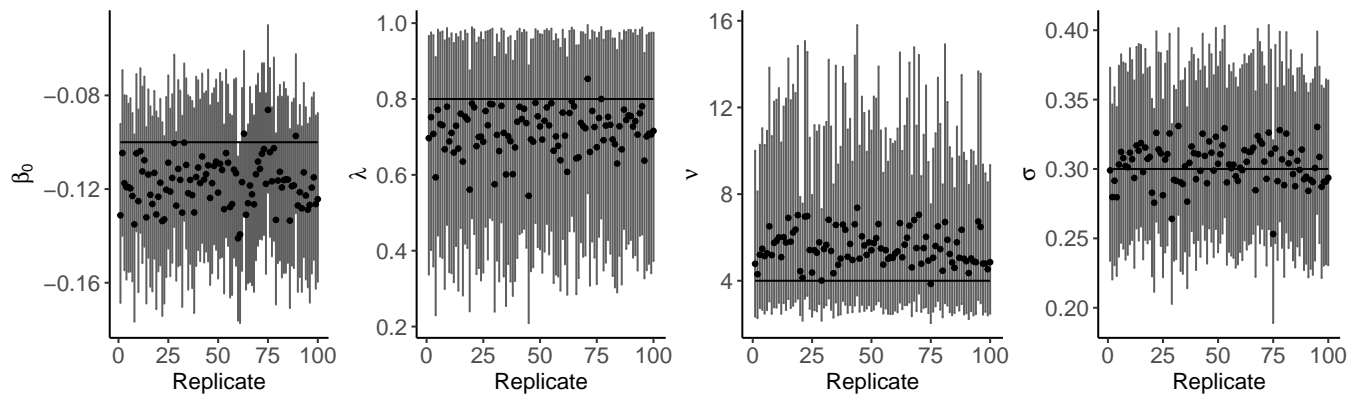


FIGURE C3 Posterior summaries of the parameters for the proposed BYM2-Gamma model across the 100 replicates regarding the simulated data from the proposed BYM2-Gamma model.

Solid circle: posterior mean; Vertical lines: 95% posterior credible interval; Solid horizontal line: true value.

Figure D6 shows that the WAIC always favours the proposed BYM2-logCAR model, which generated the data. Figure D7 shows how well the proposed BYM2-logCAR model is able to recover the true values of the model parameters through the posterior summaries across the 100 replicates for the intercept, β_0 , the mixing parameter, λ , the hyperparameter, v_κ , and the overall standard deviation, σ . Across the 100 replicates, the proposed BYM2-logCAR model always captures the truth as the posterior 95% credible intervals (vertical lines) always cover the true values of the parameters (solid horizontal lines). Regarding the scaling mixture components, κ , Figure D8 shows the estimated densities from the true κ 's (bold line) along with the ones from the first 500 MCMC iterations (gray lines) for three different replicated datasets, namely the 1st, 50th and 100th simulations. Note that the choice of the prior mean $\mu_{v_\kappa} = 0.3$ for the hyperparameter v_κ allows the κ 's to depart from 1. This departure may be towards 0, to accommodate potential outliers, as well as towards infinity. To ease visualisation, Figure D8 shows the estimated densities on a limited scale, cropping the κ 's bigger than 8. The proposed model seems to recover the true distribution of the κ 's. The proposed BYM2-logCAR model again estimates accurately the distribution of the latent effects as shown in Figure D9.

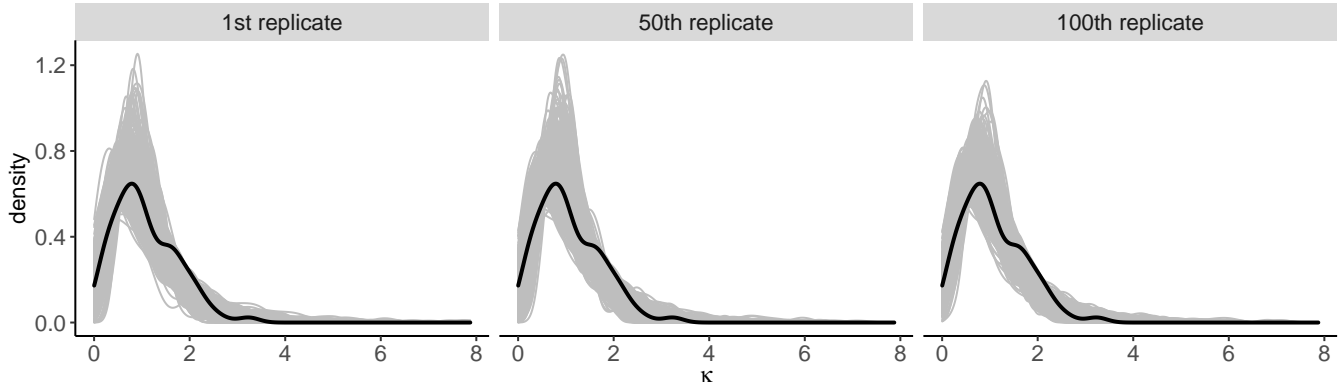


FIGURE C4 Comparison between the estimated density of the generated κ 's (solid black line) and the estimated ones from the proposed BYM2-Gamma model for the 1st, 50th and 100th replicates across the first 500 MCMC iterations (solid gray lines)

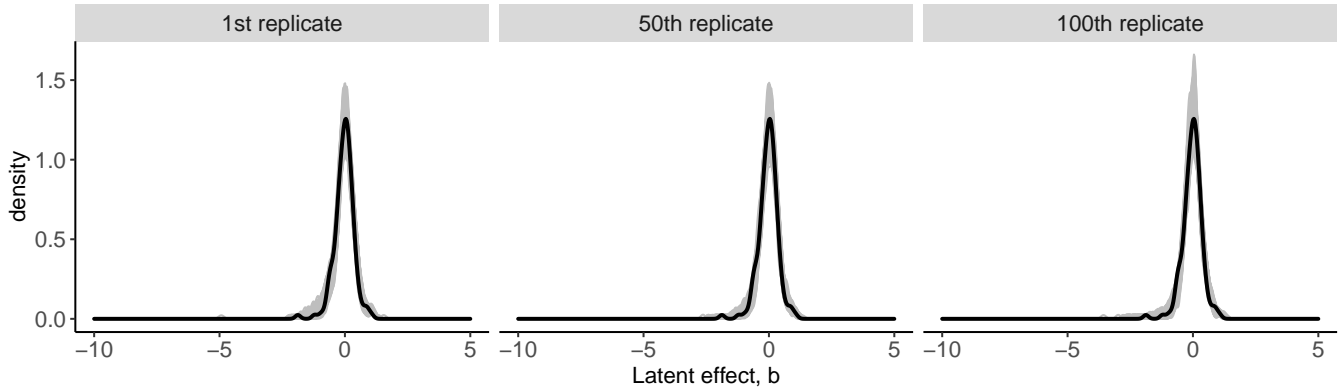


FIGURE C5 Comparison between the estimated density of the generated b 's (solid black line) and the estimated ones from the proposed BYM2-Gamma model for the 1st, 50th and 100th replicates across the first 500 MCMC iterations (solid gray lines)

E SIMULATION STUDY: NO OUTLYING AREAS

To confirm that the proposed model does not detect outliers when unnecessary, a simulation study is again conducted on the map of Rio de Janeiro without contaminating any district. Data are generated 100 times as follows:

$$Y_i \sim \mathcal{P}(E_i \exp[\beta_0 + b_i]), \quad i = 1, \dots, n,$$

with $n = 160$, $\beta_0 = -0.1$, $\mathbf{E} = [E_1, \dots, E_n]^\top$ taken from the Zika data analysis. The latent effects, $\mathbf{b} = [b_1, \dots, b_n]^\top$, are simulated once from a PCAR distribution:

$$\mathbf{b} \sim \mathcal{N}(\mathbf{0}, \sigma_b^2 [\mathbf{D} - \alpha \mathbf{W}]^{-1}),$$

with $\sigma_b = \sqrt{0.2}$ and $\alpha = 0.7$. Figure E10 shows the map of the 50th replicate of the simulated dataset, where no district seems to be an outlier with respect to the whole city. Again, the two parametrisations of the proposed model are compared to Congdon's, using the same prior distributions as described in section 3.1.

In terms of WAIC, the proposed models seem to perform best, as shown in Figure E11. For this simulation study, the interest lies particularly in comparing the outliers detections from the two versions of the proposed model and Congdon's. Figure E12 presents the districts that are found to be outliers by the BYM2-Gamma proposed model (a), the BYM2-logCAR proposed model (b) and Congdon's (c). The BYM2-Gamma model only identifies one district, Freguesia on the Governor's island, to be a potential outlier in 2% of the replicates. The BYM2-logCAR and Congdon's models on the other hand detect Freguesia up to 8% of the times, showing more sensitivity to the neighbourhood structure. Congdon's model further identifies 5 districts as potential outliers although no district was contaminated.

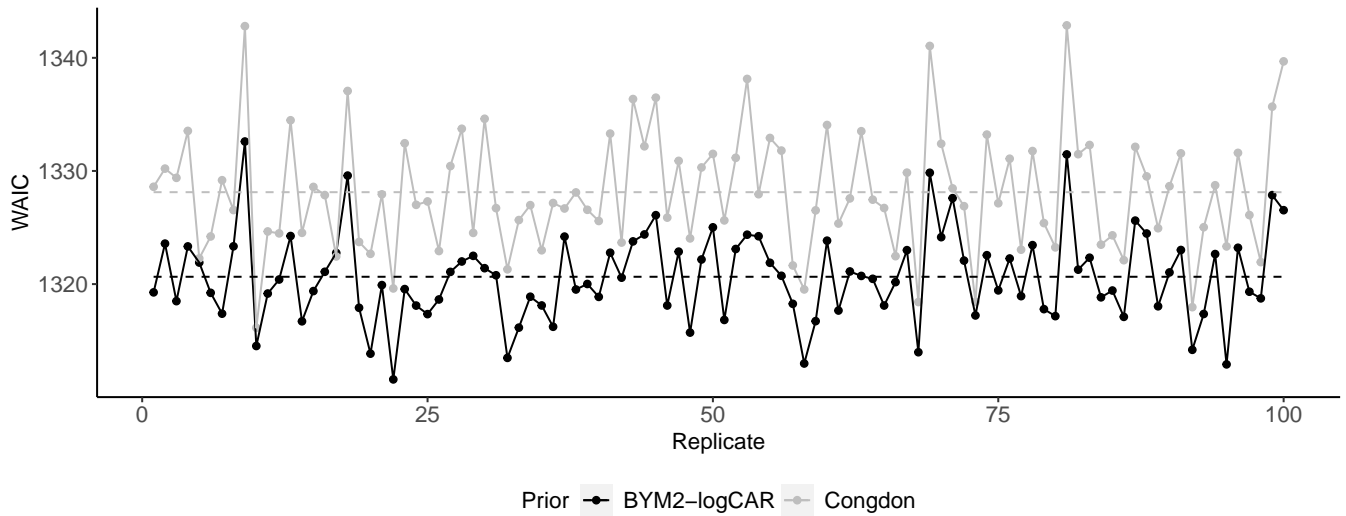


FIGURE D6 WAIC across the 100 replicates for the proposed BYM2-logCAR model and Congdon's regarding the simulated data from the proposed BYM2-logCAR model. Dashed lines: mean WAIC for each model

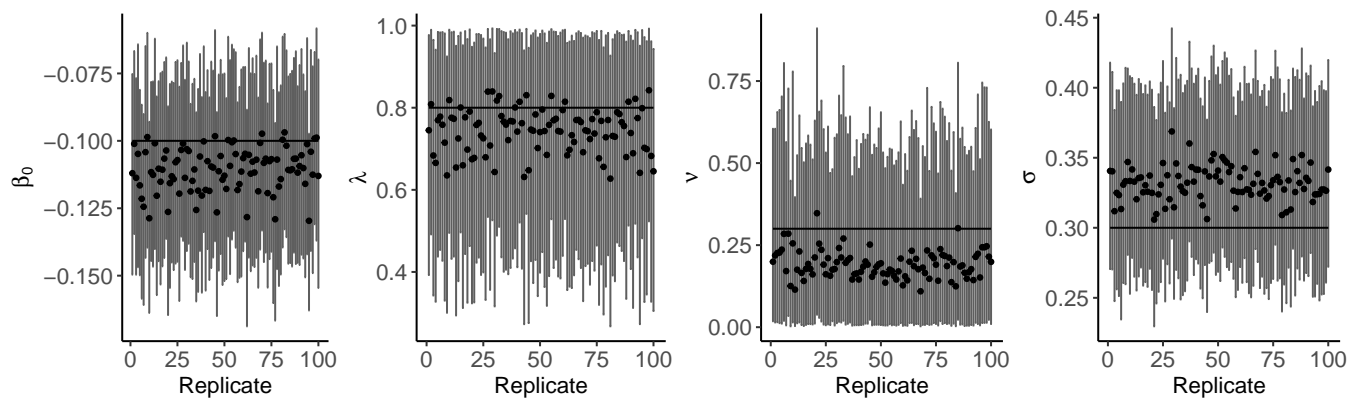


FIGURE D7 Posterior summaries of the parameters for the proposed BYM2-logCAR model across the 100 replicates regarding the simulated data from the proposed BYM2-logCAR model.

Solid circle: posterior mean; Vertical lines: 95% posterior credible interval; Solid horizontal line: true value.

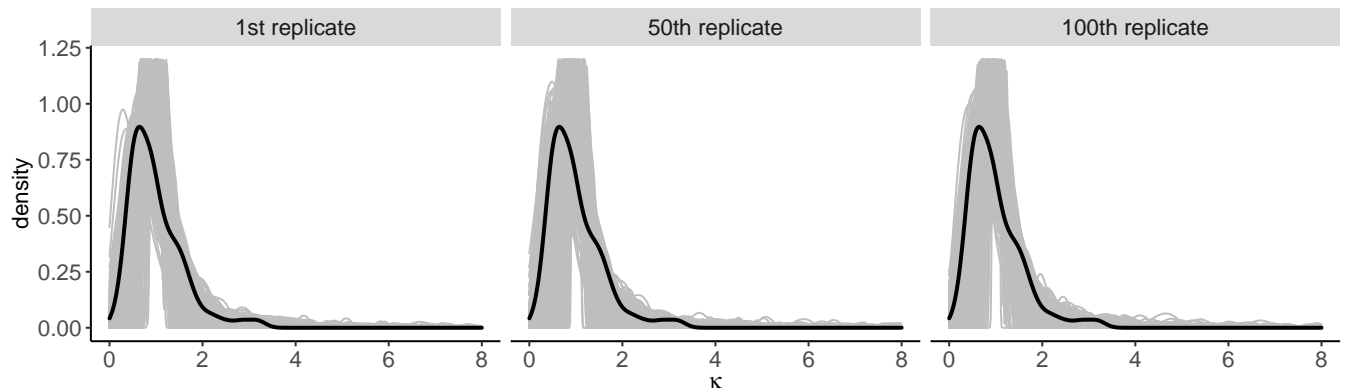


FIGURE D8 Comparison between the estimated density of the generated κ 's (solid black line) and the estimated ones from the proposed BYM2-logCAR model for the 1st, 50th and 100th replicates across the first 500 MCMC iterations (solid gray lines)

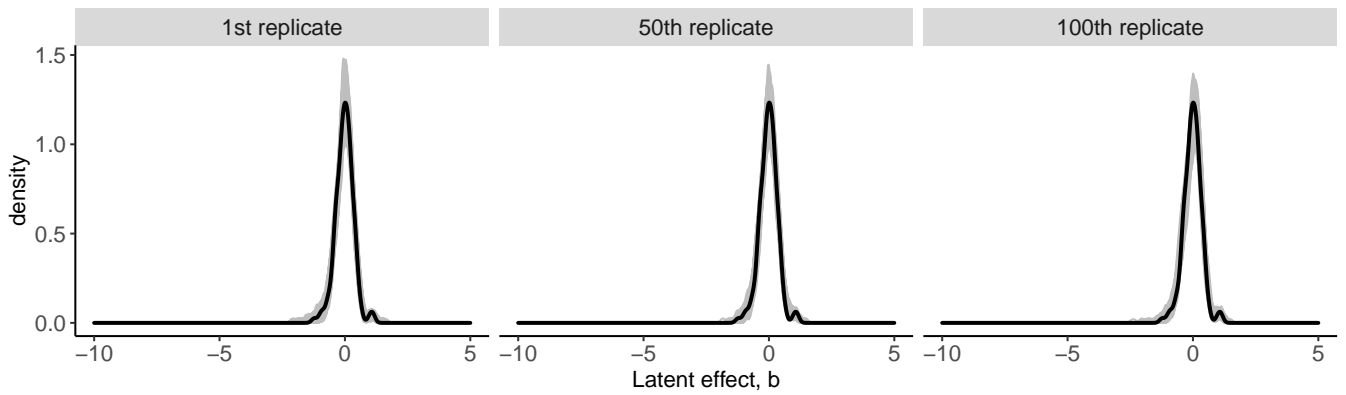


FIGURE D9 Comparison between the estimated density of the generated b 's (solid black line) and the estimated ones from the proposed BYM2-logCAR model for the 1st, 50th and 100th replicates across the first 500 MCMC iterations (solid gray lines)

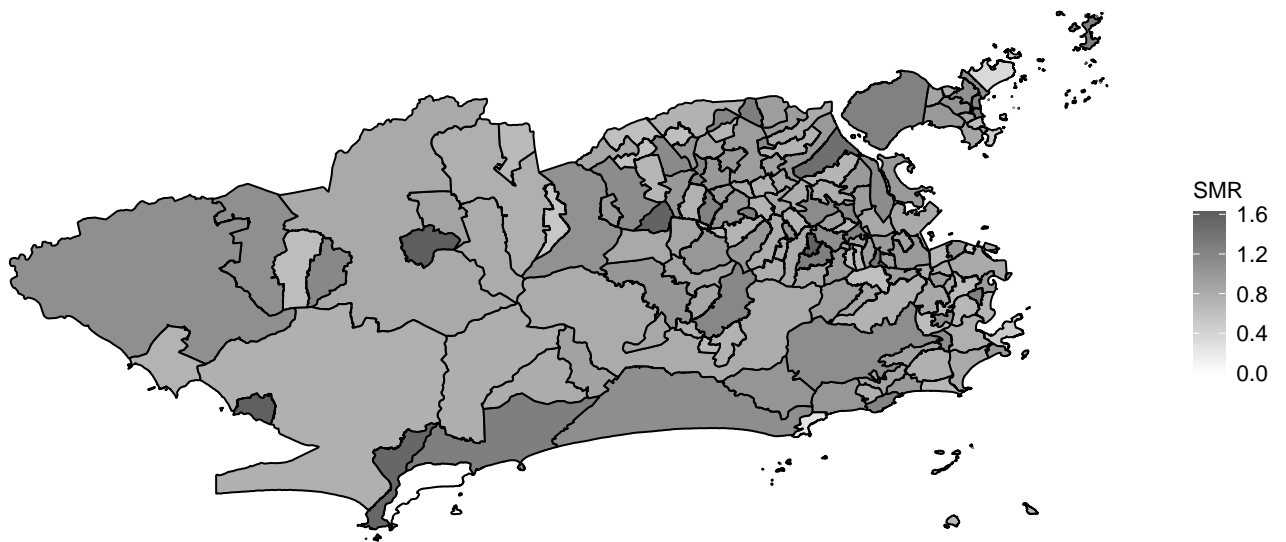


FIGURE E10 Standardised morbidity ratio for the 50th simulation without outliers.

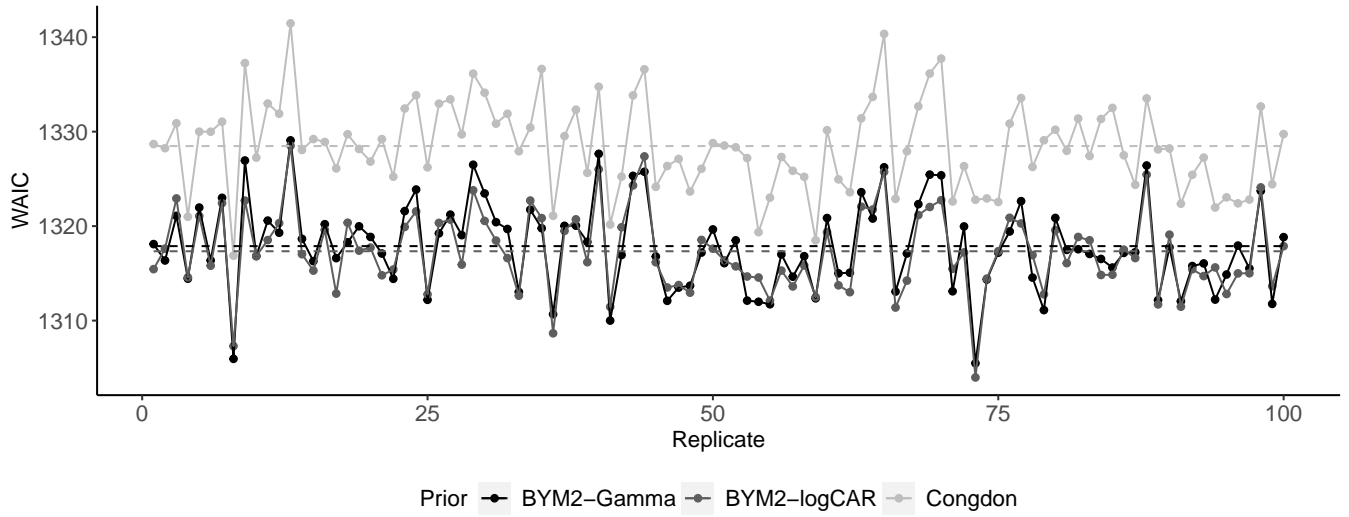


FIGURE E11 WAIC across the 100 replicates for the proposed models and Congdon's for the simulation without outliers. Dashed lines: mean WAIC for each model

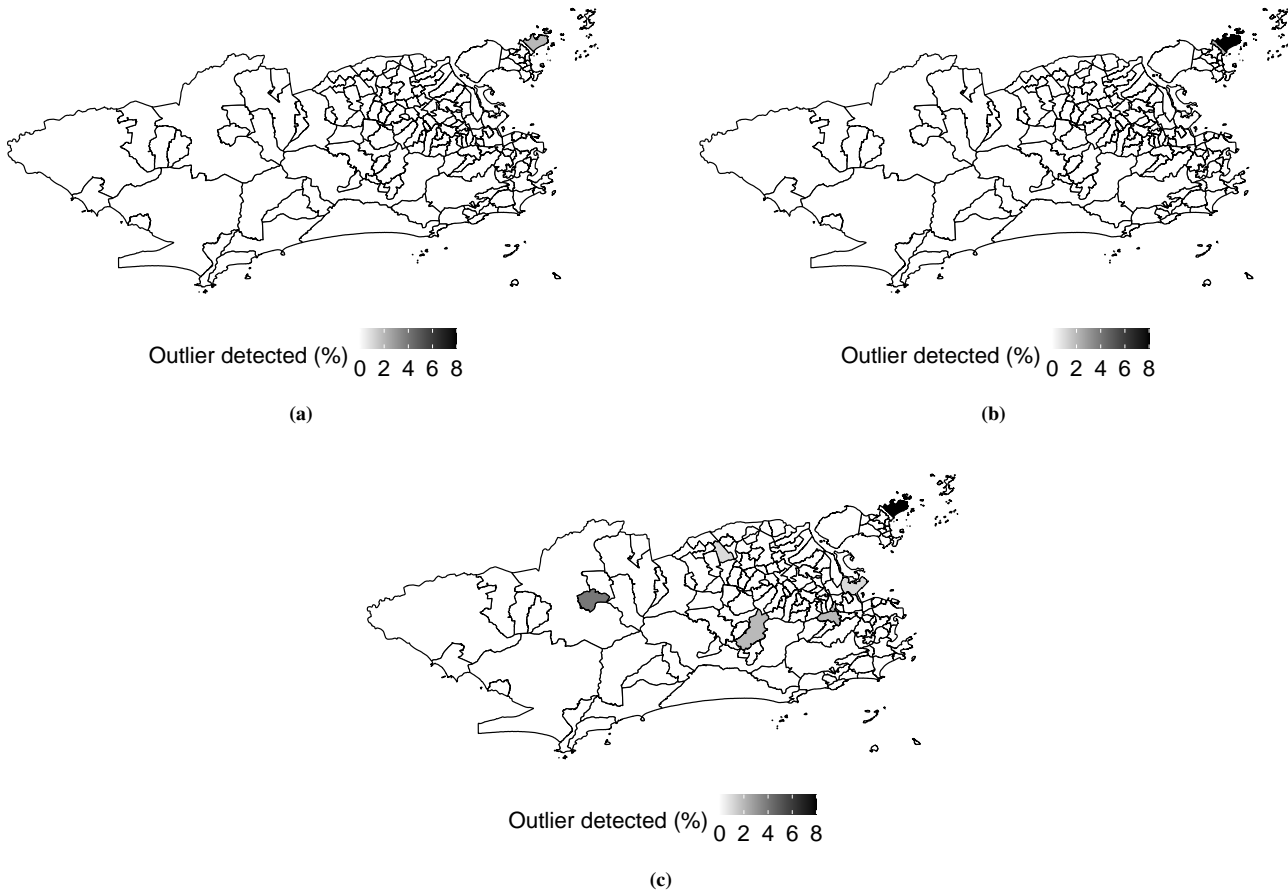


FIGURE E12 Maps of the percentages of outliers as indicated by $\kappa_{ur} < 1$ across the $r = 1, \dots, 100$ replicates, where κ_{ur} is the upper bound of the posterior 95% credible interval of κ in the r th replicate of the simulated dataset without outliers. a) BYM2-Gamma model; b) BYM2-logCAR model; c) Congdon's model.